8

VIBRATIONAL SPECTROSCOPIES AND NMR

8.0 INTRODUCTION

In this chapter, three methods for measuring the frequencies of the vibrations of chemical bonds between atoms in solids are discussed. Two of them, Fourier Transform Infrared Spectroscopy, FTIR, and Raman Spectroscopy, use infrared (IR) radiation as the probe. The third, High-Resolution Electron Energy-Loss Spectroscopy, HREELS, uses electron impact. The fourth technique, Nuclear Magnetic Resonance, NMR, is physically unrelated to the other three, involving transitions between different spin states of the atomic nucleus instead of bond vibrational states, but is included here because it provides somewhat similar information on the local bonding arrangement around an atom.

The most commonly used of these methods, and the most inexpensive, is FTIR. In it a broad band source of IR radiation is reflected from the sample (or transmitted, for thin samples). The wavelengths at which absorption occurs are identified by measuring the change in intensity of the light after reflection (transmission) as a function of wavelength. These absorption wavelengths represent excitations of vibrations of the chemical bonds and are specific to the type of bond and the group of atoms involved in the vibration. IR spectroscopy as a method of quantitative chemical identification for species in solution, or liquids, has been commercially available for 50 years. The advent of fast Fourier transform methods in conjunction with interferometer wavelength detection schemes in the last 15 years has allowed

drastic improvement in resolution, sensitivity, and reliable quantification. During this time the method has become regularly used also for solids. The sensitivity toward different bonds (chemical groups) is extremely variable, going from zero (no coupling of the IR radiation to vibrational excitations because of dipole selection rules) to high enough to detect submonolayer quantities. Intensities and line shapes are also sensitive to local solid state effects, such as stress, strain, and defects (which can therefore be characterized), so quantification is difficult, but with suitable standards 5–10% accuracy in concentrations are achievable. The depth probed depends strongly on the material (whether it is transparent or opaque to IR radiation) and can be as little as 100 Å or as much as 1 mm. The chemical nature of opaque interfaces beneath transparent overlayers can therefore be studied. Grazing angle measurements greatly reduce the probing depth, restricting it to a monolayer for molecules absorbed on metal surfaces. Often there is no spatial resolution (mm), but microfocus systems down to 20 μm exist. In Raman spectroscopy IR radiation of a single wavelength from a laser strikes the sample and the energy losses (gains) due to the Raman scattering process, which lead to some light being reemitted at lower (higher) frequencies, are determined. These loss (or gain) processes are again due to the coupling of the vibrational processes in the sample with the incident IR radiation. So, though the physics of the Raman process is quite different from that of IR spectroscopy (scattering instead of absorption), the information content is very similar. The selection rules defining which vibrational modes can be excited are different from IR, however, so Raman essentially provides complementary information. Cross sections for Raman scattering are extremely weak, resulting in Raman sensitivity being about a factor of 10 lower than for FTIR. However, better spatial resolution can be achieved (down to a few μm) because the single wavelength nature of the laser source allows an easy coupling to optical microscope elements. For the "fingerprinting" identification of chemical composition not nearly so extensive a library of data is available as for IR spectroscopy. Because of this, and because instrumentation is generally more expensive, Raman spectroscopy is less widely used, except where the microfocus capabilities are important or where differences in selection rules are critical.

Both IR and Raman have the great practical advantage of working in ambient atmosphere, and one can even study interfaces through liquids. The third vibrational technique discussed here, HREELS, requires ultrahigh vacuum conditions. A monochromatic, low-energy electron beam (a few eV) is reflected from a sample surface, losing energy by exciting vibrations (cf., Raman scattering) as it does so. Since the reflected part of the beam does not penetrate the surface, the vibrational information obtained relates only to the outermost layers. Actually two separate scattering mechanisms occur. Scattering in the specular direction is a long-range dipole process that has the same selection rules as for IR. Impact scattering is short range and nonspecular. It is an order of magnitude weaker than dipole scattering and has relaxed selection rules. Taking data in both the specular and off-specular

directions therefore maximizes the amount of information obtainable. The wavelength range accessible is wider in HREELS than in IR spectroscopy, but the resolution is orders of magnitude poorer, leading to overlapped vibrational peaks and little detailed information on individual line shapes. The major uses of HREELS have been identifying chemical species, adsorption sites, and adsorption geometries (symmetry) for monolayer adsorption at single crystal surfaces. For non-single crystal surfaces the energy-loss intensities are drastically reduced, but the technique is still useful. It has been quite extensively used for characterizing polymer surfaces. For insulators charging can sometimes be a problem.

The last technique discussed here, NMR, involves immersing the sample in a strong magnetic field (1–12 Tesla), thereby splitting the degeneracy of the spin states of those nuclei that have either an odd mass or odd atomic number and hence possess a permanent magnetic moment. About half the elements in the periodic table have isotopes fulfilling these conditions. Excitation between these magnetic levels is then performed by absorption of radiofrequency (RF) radiation. By measuring the energy at which the absorptions occur (the "resonance" energies) the energy differences between the spin (magnetic) states are determined. For any given magnetic field the values are element specific, but the nuclear magnetic moments and electronic environment surrounding the target atoms also exert an influence, splitting the absorption resonances into multiple lines and shifting peak positions. From these effects the local environment of the atoms concerned—the coordination number, local symmetries, the nature of neighboring chemical groups, and bond distances—can be studied. H-atom NMR has been used as an analytical tool for molecules in liquids for about 40 years to identify chemical groupings, and the sequence of groupings containing H atoms. It is also, of course, the basis of Magnetic Resonance Imaging, MRI, which is used medically. In the solid state, crystalline phases can be identified, and quantitative analysis can be achieved directly in mixtures from the relative intensities of peaks and the use of well-defined model compound standards. In many cases the NMR spectra of solids are rather broad and unresolved due to strong anisotropic effects with respect to the applied magnetic field. There are a number of ways of removing these effects, the most popular being magic-angle spinning of the sample, which can collapse broad powder patterns into sharp resonances that can be easily assigned. NMR is intrinsically a bulk technique; the signal comes from the entire sample which is immersed in the magnetic field. At least 10 mg of material is required (powders, thin films, or crystals), and to get any information specific to surfaces or interfaces requires large surface areas (10–150 m^2/gm). Costs vary a lot ($200,000 to $1,200,000), depending on how wide a range of elements needs to be accessed, since this determines the range and magnitude of the magnetic fields and RF capabilities required.

8.1 FTIR

Fourier Transform Infrared Spectroscopy

J. NEAL COX

Contents

Introduction

The physical principles underlying infrared spectroscopy have been appreciated for more than a century. As one of the few techniques that can provide information about the chemical bonding in a material, it is particularly useful for the nondestructive analysis of solids and thin films, for which there are few alternative methods. Liquids and gases are also commonly studied, more often in conjunction with other techniques. Chemical bonds vary widely in their sensitivity to probing by infrared techniques. For example, carbon-sulfur bonds often give no infrared signal, and so cannot be detected at any concentration, while silicon-oxygen bonds can produce signals intense enough to be detected when probing submonolayer quantities, or on the order of 10^{13} bonds/cc. Thus, the potential utility of infrared spectrophotometry (IR) is a function of the chemical bond of interest, rather than being applicable as a generic probe. For quantitative analysis, modern instrumentation can provide a measurement repeatability of better than 0.1%. Accuracy and precision, however, are more commonly on the order of 5.0% (3σ), relative. The limitations arise from sample-to-sample variations that modify the optical quality of the material. This causes slight, complex distortions of the spectrum that are dif-

ficult to eliminate. Sensitivity of the sample to environmental influences that modify the chemical bonding and the need to calibrate the infrared spectral data to reference methods—such as neutron activation, gravimetry, and wet chemistry—also tend to degrade slightly the measurement for quantitative work.

The goal of the basic infrared experiment is to determine changes in the intensity of a beam of infrared radiation as a function of wavelength or frequency (2.5–50 μm or 4000–200 cm^{-1}, respectively) after it interacts with the sample. The centerpiece of most equipment configurations is the infrared spectrophotometer. Its function is to disperse the light from a broadband infrared source and to measure its intensity at each frequency. The ratio of the intensity before and after the light interacts with the sample is determined. The plot of this ratio versus frequency is the *infrared spectrum.*

As technology has progressed over the last 50 years, the infrared spectrophotometer has passed through two major stages of development. These phases have significantly impacted how infrared spectroscopy has been used to study materials. Driven in part by the needs of the petroleum industry, the first commercial infrared spectrophotometers became available in the 1940s. The instruments developed at that time are referred to as *spatially dispersive* (sometimes shortened to *dispersive*) instruments because ruled gratings were used to disperse spatially the broadband light into its spectral components. Many such instruments are still being built today. While somewhat limited in their ability to provide quantitative data, these dispersive instruments are valued for providing qualitative chemical identification of materials at a low cost. The 1970s witnessed the second phase of development. A new (albeit much more expensive) type of spectrophotometer, which incorporated a Michelson interferometer as the dispersing element, gained increasing acceptance. All frequencies emitted by the interferometer follow the same optical path, but differ in the time at which they are emitted. Thus these systems are referred to as being *temporally dispersive.* Since the intensity-time output of the interferometer must be subjected to a Fourier transform to convert it to the familiar infrared spectrum (intensity-frequency), these new units were termed Fourier Transform Infrared spectrophotometers, (FTIR). Signal-to-noise ratios that are higher by orders of magnitude, much better resolution, superior wavelength accuracy, and significantly shorter data acquisition times are gained by switching to an interferometer. This had been recognized for several decades, but commercialization of the equipment had to await the arrival of local computer systems with significant amounts of cheap memory, advances in equipment interfacing technology, and developments in fast Fourier-transform algorithms and circuitry.

Beyond the complexities of the dispersive element, the equipment requirements of infrared instrumentation are quite simple. The optical path is normally under a purge of dry nitrogen at atmospheric pressure; thus, no complicated vacuum pumps, chambers, or seals are needed. The infrared light source can be cooled by water. No high-voltage connections are required. A variety of detectors are avail-

able, with deuterated tri-glycene sulfate (DTGS) detectors offering a good signal-to-noise ratio and linearity when operated at room temperature. For more demanding applications, the mercury cadmium telluride (HgCdTe, or mer-cad telluride) detector, cooled by liquid nitrogen, can be used for a factor-of-ten gain in sensitivity.

With the advent of FTIR instrumentation, IR has experienced a dramatic increase in applications since the 1970s, especially in the area of quantitative analysis. FTIR spectrophotometry has grown to dominate the field of infrared spectroscopy. Experiments in microanalysis, surface chemistry, and ultra-thin films are now much more routine. The same is true for interfaces, if the infrared characteristics of the exterior layers are suitable. While infrared methods still are rarely used to profile composition as a function of depth, microprobing techniques available with FTIR technology permit the examination of microparticles and *xy*-profiling with a spatial resolution down to 20 μm. Concurrent with opening the field to new areas of research, the high level of computer integration, coupled with robust and nondestructive equipment configurations, has accelerated the move of the instrument out of the laboratory. Examples are in VLSI, computer-disk, and chemicals manufacturing, where it is used as a tool for thin-film, surface coating, and bulk monitors.

Unambiguous chemical identification usually requires the use of other techniques in conjunction with IR. For gases and liquids, Mass Spectrometry (MS) and Nuclear Magnetic Resonance Spectrometry (NMR) are routinely employed. The former, requiring only trace quantities of material, determines the masses of the molecule and of characteristic fragments, which can be used to deduce the most likely structure. MS data is sometimes supplemented with infrared results to distinguish certain chemical configurations that might produce similar fragment patterns. NMR generally requires a few milliliters of sample, more than needed by either the FTIR or MS techniques, and can identify chemical bonds that are associated with certain elements, bonds that are adjacent to each other, and their relative concentrations. Solids can also be studied by these methods. For MS, the sensitivity remains high, but the method is destructive because the solid must somehow be vaporized. While nondestructive, the sensitivity of NMR spectrometry is typically much lower for direct measurements on solids; otherwise, the solid may be taken into solution and analyzed. For thin films, both the MS and NMR methods are destructive. Complementary data for surfaces, interfaces, and thin films can be obtained by techniques like X-ray photoelectron spectroscopy, static secondary ion mass spectrometry, and electron energy loss spectrometry. These methods probe only the top few nanometers of the material. Depending upon the sample and the experimental configuration, IR may be used as either a surface or a bulk probe for thin films. For surface analysis, FTIR is about a factor of 10 less sensitive than these alternative methods. Raman spectroscopy is an optical technique that is complementary to infrared methods and also detects the vibrational motion of chemical bonds. While able to achieve submicron spatial resolution, the sensitivity of the

Raman technique is usually more than an order of magnitude less than that of FTIR.

As a surface probe, FTIR works best when the goal is to study a thin layer of material on a dissimilar substrate. Lubricating oil on a metal surface and thin oxide layers on semiconductor surfaces are examples. FTIR techniques become more difficult to apply when the goal is to examine a surface or layer on a similar substrate. An example would be the study of thin skins or surface layers formed during the curing cycles used for photoresist or other organic thin films deposited from the liquid phase. If the curing causes major changes in the bulk and the surface, FTIR methods usually cannot discriminate between them, because the beam probes deeply into the bulk material. The limitations as a surface probe often are dictated by the type of substrate being used. A metal or high refractive-index substrate will reflect enough light to permit sensitive probing of the surface region. A low refractive index substrate, in contrast, will permit the beam to probe deeply into the bulk, degrading the sensitivity to the surface.

The discussions presented in this article pertain to applications of FTIR, because most of the recent developments in the field have been attendant to FTIR technology. In many respects, FTIR is a "science of accessories". A myriad of sample holders, designed to permit the infrared light to interact with a given type of sample in an appropriate manner, are interfaced to the spectrophotometer. A large variety of "hyphenated" techniques, such as GC-FTIR (gas chromatography-FTIR) and TGA-FTIR (thermo-gravimetric analysis-FTIR), also are used. In these cases, the effluent emitted by the GC, TGA, or other unit is directed into the FTIR system for time-dependent study. Hyphenated methods will not be discussed further here. Still, common to all of these methods is the goal of obtaining and analyzing an infrared spectrum.

Basic Principles

Infrared Spectrum

Define I_0 to be the intensity of the light incident upon the sample and I to be the intensity of the beam after it has interacted with the sample. The goal of the basic infrared experiment is to determine the intensity ratio I/I_0 as a function of the frequency of the light (w). A plot of this ratio versus the frequency is the infrared spectrum. The infrared spectrum is commonly plotted in one of three formats: as transmittance, reflectance, or absorbance. If one is measuring the fraction of light transmitted through the sample, this ratio is defined as

$$T_w = \left(\frac{I_t}{I_0}\right)_w \tag{1}$$

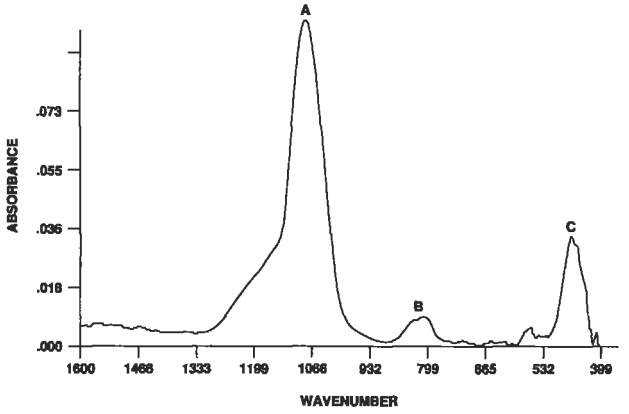

Figure 1 **The FTIR spectrum of the oxide of silicon (thin film deposited by CVD). Primary features: (a), asymmetric stretching mode of vibration; (b), bending mode of vibration; (c), rocking mode of vibration.**

where T_w is the transmittance of the sample at frequency w, and I_t is the intensity of the transmitted light. Similarly, if one is measuring the light reflected from the surface of the sample, then the ratio is equated to R_w, or the reflectance of the spectrum, with I_t being replaced with the intensity of the reflected light I_r. The third format, absorbance, is related to transmittance by the Beer-Lambert Law:

$$A_w = -\log T_w = (\varepsilon_w)(bc) \tag{2}$$

where c is the concentration of chemical bonds responsible for the absorption of infrared radiation, b is the sample thickness, and ε_w is the frequency-dependent absorptivity, a proportionality constant that must be experimentally determined at each w by measuring the absorbance of samples with known values of bc. As a first-order approximation the Beer-Lambert Law provides an simple foundation for quantitating FTIR spectra. For this reason, it is easier to obtain quantitative results if one collects an absorbance spectrum, as opposed to a reflectance spectrum. Prior to the introduction of FTIR spectrophotometers, infrared spectra were usually published in the transmittance format, because the goal of the experiment was to obtain qualitative information. With the growing use of FTIR technology, a quantitative result is more often the goal. Today the absorbance format dominates, because to first order it is a linear function of concentration.

Qualitative and Quantitative Analysis

Figure 1 shows a segment of the FTIR absorbance spectrum of a thin film of the oxide of silicon deposited by chemical vapor deposition techniques. In this film, sil-

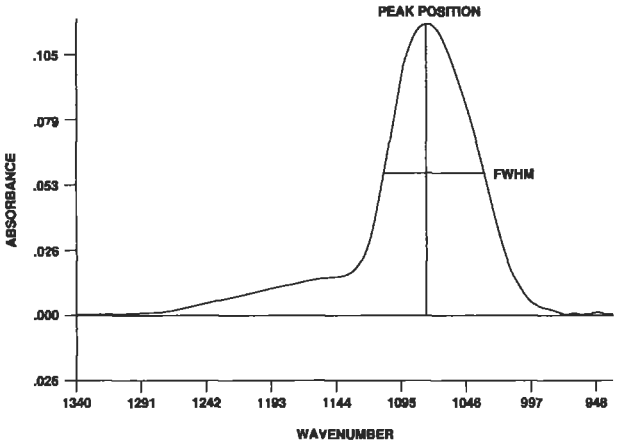

Figure 2 **Spectral parameters typically used in band shape analysis of an FTIR spectrum: peak position, integrated peak area, and FWHM.**

icon is tetrahedrally coordinated with four bridging oxygen atoms. Even though the bond angles are distorted slightly to produce the random glassy structure, this spectrum is quite similar to that obtained from crystalline quartz, because most features in the FTIR spectrum are the result of nearest neighbor interactions. In crystalline materials the many vibrational modes can be classified by the symmetry of their motions and, while not rigorous, these assignments can be applied to the glassy material, as well. Thus the peak near 1065 cm^{-1} arises from the asymmetric stretching motions of the Si and O atoms relative to each other. The band near 815 cm^{-1} arises from bending motions, while the one near 420 cm^{-1} comes from a collective rocking motion. These are not the only vibrational modes for the glass, but they are the only ones that generate electric dipoles that are effective in coupling with the electromagnetic field. For example, the glass also has a symmetric stretching mode, but since it generates no net dipole, no absorption band appears in the FTIR spectrum. For more quantitative work, the fundamental theory of infrared spectroscopy delineates a band shape analysis illustrated in Figure 2. Three characteristics are commonly examined: peak position, integrated peak intensity, and peak width.

Peak position is most commonly exploited for qualitative identification, because each chemical functional group displays peaks at a unique set of characteristic frequencies. The starting point for such a functional-group analysis is a table or computer database of peak positions and some relative intensity information. This provides a fingerprint that can be used to identify chemical groups. Thus the three peaks just described for the oxide of silicon can be used to identify that material. Typical of organic materials, C–H bonds have stretching modes around 3200 cm^{-1}; C = O, around 1700 cm^{-1}. Thus, the composition of oils may be qualitatively identified by classifying these and other peak positions observed in the spectrum. In

addition, some bands have positions that are sensitive to physicomechanical properties. As a result, applied and internal pressures, stresses, and bond strain due to swelling can be studied.

The Beer-Lambert Law of Equation (2) is a simplification of the analysis of the second-band shape characteristic, the integrated peak intensity. If a band arises from a particular vibrational mode, then to the first order the integrated intensity is proportional to the concentration of absorbing bonds. When one assumes that the area is proportional to the peak intensity, Equation (2) applies.

In solids and liquids, peak width—the third characteristic—is a function of the homogeneity of the chemical bonding. For the most part, factors like defects and bond strain are the major sources of band width, usually expressed as the full width at half maximum (FWHM). This is due to the small changes these factors cause in the strengths of the chemical bonds. Small shifts in bond strengths cause small shifts in peak positions. The net result is a broadening of the absorption band. The effect of curing a material can be observed by peak-width analysis. As one anneals defects the bands become narrower and more intense (to conserve area, if no bonds are created or destroyed). Beyond the standard analysis, higher order band shape properties may also be examined, such as peak asymmetry. For example, the apparent shoulder on the high-frequency side of the band in Figure 2 may be due to a second band that overlaps the more prominent feature.

For many applications, quantitative band shape analysis is difficult to apply. Bands may be numerous or may overlap, the optical transmission properties of the film or host matrix may distort features, and features may be indistinct. If one can prepare samples of known properties and collect the FTIR spectra, then it is possible to produce a calibration matrix that can be used to assist in predicting these properties in unknown samples. Statistical, chemometric techniques, such as PLS (partial least-squares) and PCR (principle components of regression), may be applied to this matrix. Chemometric methods permit much larger segments of the spectra to be comprehended in developing an analysis model than is usually the case for simple band shape analyses.

Methodologies and Accessories

A large number of methods and accessories have been developed to permit the infrared source to interact with the sample in appropriate ways. Some of the more common approaches are listed below.

Single-pass transmission

The direct transmission experiment is the most elegant and yields the most quantifiable results. The beam makes a single pass through the sample before reaching the detector. The bands of interest in the absorbance spectrum should have peak absorbances in the range of 0.1–2.0 for routine work, although much weaker or stronger bands can be studied. Various holders, pellet presses, and liquid cells have been

developed to permit samples to be prepared with the appropriate path length. *Diamond anvil cells* permit pliable samples to be squeezed to extremely thin path lengths or to be studied under applied pressures. Long path-length cells are used for samples in the gas phase. Thin films and prepared surfaces can be studied by transmission if the supporting substrate is transparent to the infrared. The highest sensitivity is obtained with double-beam or pseudo-double-beam experimental configurations. An example of the latter is the *interleaf* experiment, where a single beam is used, but a sample and reference are alternately shuttled into and out of the beam path.

Reflection

If the sample is inappropriate for a transmission experiment, for instance if the supporting substrate is opaque, a reflectance configuration will often be employed. Accessories to permit specular, diffuse, variable-angle, and grazing-incidence experiments are available. The angle of incidence can be adjusted to minimize multiple-reflection interferences by working at the Bragg angle for thin films, or to enhance the sensitivity of the probe to surface layers. A subset of this technique, Reflection Absorption (RA) spectroscopy, is capable of detecting submonolayer quantities of materials on metal surfaces. These grazing and RA techniques can enhance surface sensitivities by using geometries that optimize the coupling of the electromagnetic field at the metal surface. In some instances it has been possible to deduce preferred molecular orientations of ordered monolayers.

Attenuated Total Reflection

In this configuration an Attenuated Total Reflection (ATR) crystal is used, illustrated in Figure 3. The infrared beam is directed into the crystal. Exploiting the principles of a waveguide, the change in refractive index at the crystal surface causes the beam to be back-reflected several times as it propagates down the length of the crystal before it finally exits to the detector. If the sample is put into contact with the crystal surface, the beam will interact weakly with the sample at several points. For extremely thin samples, this is a means of increasing the effective path length. Since the propagating beam in the crystal barely penetrates through the surface of the sample adjacent to the crystal, signals at a sample surface can be enhanced, as well. This also helps in the study of opaque samples. Approximately fivefold amplifications in signals are typical over a direct transmission experiment. The quality of the crystal–sample interface is critical, and variability in that interface can make ATR results very difficult to quantify.

Emission

When samples are heated, they emit infrared radiation with a characteristic spectrum. The IR emission of ceramics, coals, and other complicated solids and thin films can be studied. Also, if conditions make it difficult to use an infrared source

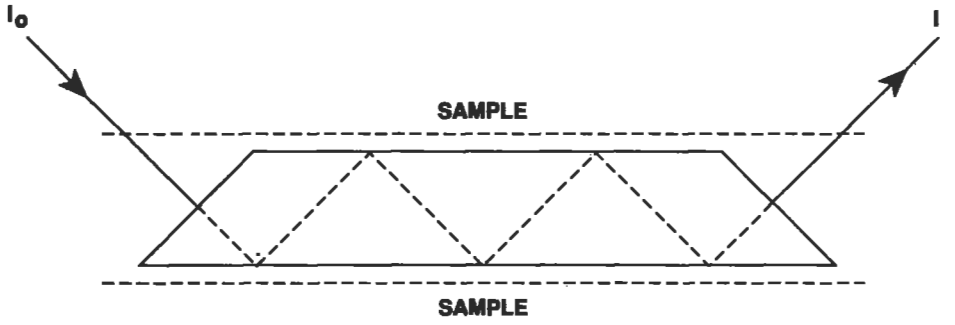

Figure 3 **Typical beam path configuration for collecting an FTIR spectrum using an attenuated total reflectance element: I_0 is the incident infrared beam, I is the exiting beam.**

(such as an *in situ* measurement of a thin film in the deposition chamber) but permit the controlled heating of a sample, then emission methods provide a means of examining these materials.

Microscopy

Infrared microscopes can focus the beam down to a 20-μm spot size for microprobing in either the transmission or reflection mode. Trace analysis, microparticle analysis, and spatial profiling can be performed routinely.

Interferences and Artifacts

Equipment

Equipment technology and processing software for FTIR are very robust and provide a high degree of reliability. Concerns arise for only the most demanding applications. For quantitative work on an isolated feature in the spectrum, the rule of thumb is that the spectrometer resolution be one-tenth the width of the band. FTIR instruments routinely meet that requirement for solids.

Short- and long-term drift in the spectral output can be caused by several factors: drift in the output of the infrared light source or of the electronics, aging of the beam splitter, and changes in the levels of contaminants (water, CO_2, etc.) in the optical path. These problems are normally eliminated by rapid, routine calibration procedures.

The two complicating factors that are encountered most frequently are the linearity of detector response and stray light scattering at low signal levels. DTGS

detectors are quite linear and reliable, while MCT detectors can saturate at relatively low light levels. Stray light can make its way to the detector and be erroneously detected as signal, or it can be backscattered into the interferometer and degrade its output. A problem only at very low signal levels or with very reflective surfaces, proper procedures can minimize these effects.

Intrinsic or Matrix

Few cross sections for infrared absorption transitions have been published and typically they are not broadly applicable. The strength of the absorption depends upon changes in the dipole moment of the material during the vibrational motion of the constituent atoms. However, these moments are also very sensitive to environmental factors, such as nearest neighbor effects, that can cause marked changes in the infrared spectrum. For example, carbon–halogen bonds have a stretching mode that may be driven from a being very prominent feature to being an undetectable feature in the spectrum by adding electron-donating or -withdrawing substituents as nearest neighbors. For careful quantitative work, then, model compounds that are closely representative of the material in question are often needed for calibration.

Interface Optical Effects

For thin-film samples, abrupt changes in refractive indices at interfaces give rise to several complicated *multiple reflection* effects. Baselines become distorted into complex, sinusoidal, fringing patterns, and the intensities of absorption bands can be distorted by multiple reflections of the probe beam. These artifacts are difficult to model realistically and at present are probably the greatest limiters for quantitative work in thin films. Note, however, that these interferences are functions of the complex refractive index, thickness, and morphology of the layers. Thus, properly analyzed, useful information beyond that of chemical bonding potentially may be extracted from the FTIR spectra.

Many materials have grain boundaries or other microstructural features on the order of a micrometer or greater. This is on the same scale as the wavelength of the infrared radiation, and so artifacts due to the wavelength-dependent scattering of light at these boundaries can be introduced into the spectra. Thin films, powders, and solids with rough surfaces are the most affected. Again these artifacts are difficult to realistically model, but properly analyzed can provide additional information about the sample.

Conclusions

The principles of infrared spectroscopy can be exploited to extract information on the chemical bonding of an extremely wide variety of materials. The greatest strength of the technique is as a nondestructive, bulk probe of glassy and amor-

phous materials, where few alternate methods exist for obtaining chemical information. For other materials, FTIR is a valuable member in the arsenal of characterization tools. Other methods that are most likely to provide similar information include raman spectroscopy, X-ray photoelectron spectroscopy, NMR, MS, SIMS, and high-resolution electron energy-loss spectroscopy. The nondestructive, noninvasive potential of the infrared technique, and its ease of use, continues to distinguish it from these other methods, with the exception of Raman spectroscopy.

The trends begun with the general introduction of FTIR technology will undoubtedly continue. It is safe to say that the quality of the data being produced far exceeds our ability to analyze it. In fact, for many current applications, the principle limitations are not with the equipment, but rather with the quality of the samples. Thus, the shift from qualitative to quantitative work will proceed, reaching high levels of sophistication to address the optical and matrix interference problems discussed above.

With extensive computerization, the ease of use, and the robustness of equipment, movement of the instrumentation from the research laboratory to the manufacturing environment, for application as *in situ* and at-line monitors, will continue. *In situ* work in the research laboratory will also grow. New environments for application appear every day and improved computer-based data processing techniques make the rapid analysis of large sets of data more commonplace. These developments, coupled with rapid data acquisition times, are making possible the timely evaluation of the results of large-scale experiments. Most likely, much of the new physicochemical information developed by applying FTIR technology will come from trends observed in detailed studies of these large sample data sets.

Related Articles in the Encyclopedia

Raman Spectroscopy and HREELS

References

1 B. George and P. McIntyre. *Analytical Chemistry by Open Learning: Infrared Spectroscopy.* John Wiley & Sons, New York, 1987. A good primer on the basics of applied infrared spectroscopy.

2 P. R. Griffiths and J. A. de Haseth. *Fourier Transform Infrared Spectrometry.* John Wiley & Sons, New York, 1986. Chapters 1–8 review FTIR equipment in considerable detail. Chapters 9–19 describe applications, including surface techniques (Chapter 17).

3 *Practical Fourier Transform Infrared Spectroscopy: Industrial and Laboratory Chemical Analysis.*(J. R. Ferraro and K. Krishnan, eds.) Academic Press, New York, 1990. Chapters 3 (by K. Krishnan and S. L. Hill) and

Chapter 7 (by H. Ishida and A. Ishitani) review microscopic and surface analytical techniques. Chapter 8 (by D. M. Haaland) reviews developments in statistical chemometrics for data analysis.

4 O. S. Heavens. *Optical Properties of Thin Solid Films.* Butterworths, 1955. Chapter 4 presents a detailed mathematical description of the Fresnel fringing phenomenon for the transmission of light through thin films.

5 C. F. Bohren and D. R. Huffman. *Absorption and Scattering of Light by Small Particles.* John Wiley & Sons, New York, 1983. Parts 1 and 2 describe the theory of the scattering problem in some detail. Part 3 compares theory with experiment.

8.2 Raman Spectroscopy

WILLIAM B. WHITE

Contents

Introduction

To a surprisingly accurate approximation, molecules and crystals can be thought of as systems of balls (atoms) connected by springs (chemical bonds). These systems can be set into vibration, and vibrate with frequencies determined by the mass of the balls (atomic weights) and by the stiffness of the springs (bond force constants). Diatomic molecules (O_2, CO, HCl, etc.) having two balls connected by a single spring have only one fundamental vibrational frequency. The same is true for diatomic crystals, which have a single diatomic formula unit in the primitive unit cell (NaCl, ZnS, diamond, etc.), although the details are more complicated. The number of possible vibrational motions is $3n-6$ for nonlinear molecules and $3n-3$ for crystals, where n is the number of atoms in the molecule or in the primitive unit cell of the crystal. The mechanical molecular and crystal vibrations are at very high frequencies, in the range 10^{12}–10^{14} Hz (3–300 μm wavelength), which places them in the infrared (IR) region of the electromagnetic spectrum. Coupling between incident infrared radiation and the electronic structure of the chemical bond produces the infrared absorption spectrum as a direct means of observing molecular

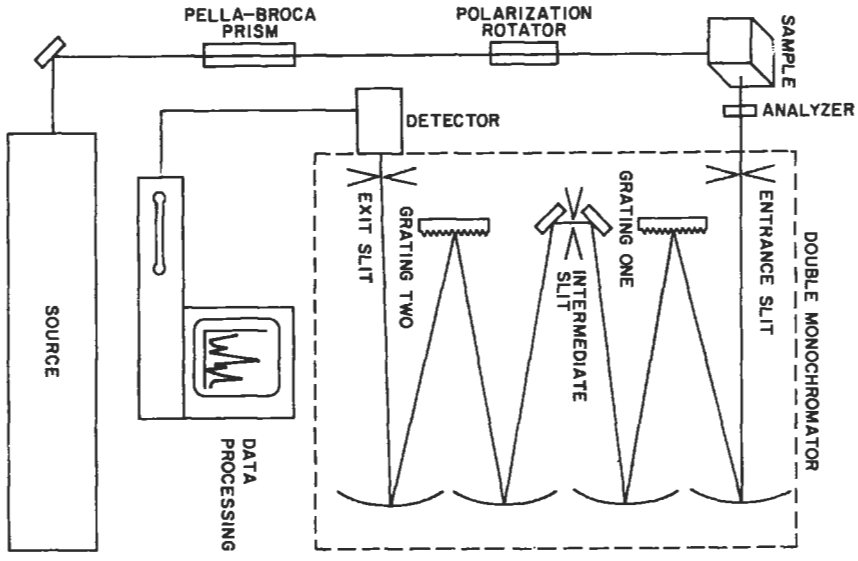

Figure 1 **Drawing of single-channel Raman spectrometer showing Czerny–Turner type double monochromator. Collecting optics for scattered beam are not shown.**

and crystal vibrations (see the article on FTIR). The Raman spectrum arises from an indirect coupling of high-frequency radiation (usually visible light, but also ultraviolet and near infrared) with the electron clouds that make up the chemical bonds. Thus, although both IR absorption and Raman spectroscopy measure the vibrational spectra of materials, the physical processes are different, the selection rules that determine which of the vibrational modes are excited are different, and the two spectroscopies must be considered to be complementary. Both, however, are characterization probes that are sensitive to the details of atomic arrangement and chemical bonding.

Raman spectroscopy is primarily a structural characterization tool. The spectrum is more sensitive to the lengths, strengths, and arrangement of bonds in a material than it is to the chemical composition. The Raman spectrum of crystals likewise responds more to details of defects and disorder than to trace impurities and related chemical imperfections.

Basic Principles

The essentials of the Raman scattering experiment are shown in Figure 1. An intense monochromatic light beam impinges on the sample. The electric field of the incident radiation distorts the electron clouds that make up the chemical bonds in the sample, storing some energy. When the field reverses as the wave passes, the

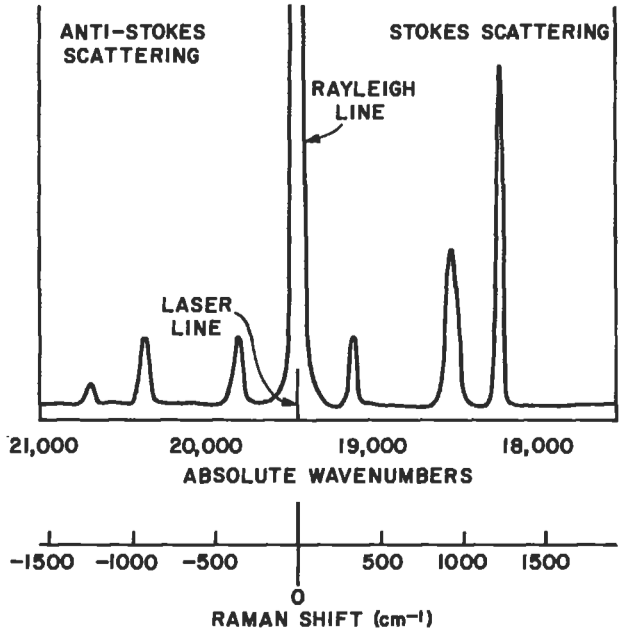

Figure 2 **Schematic Raman scattering spectrum showing Rayleigh line, Stokes Raman scattering and anti-Stokes Raman scattering. Note arrangements of wavenumber scales with Rayleigh line defining the zero on the Raman wavenumber scale.**

distorted electron clouds relax and the stored energy is reradiated. Although the incident beam may be polarized so that the electric field is oriented in a specific direction with respect to the sample, the scattered beam is reradiated in all directions, making possible a variety of scattering geometries. Most of the stored energy is reradiated at the same frequency as that of the incident exciting light. This component is known as the Rayleigh scattering and gives a strong central line in the scattering spectrum (Figure 2). However, a small portion of the stored energy is transferred to the sample itself, exciting the vibrational modes. The vibrational energies are deducted from the energy of the incident beam and weak side bands appear in the spectrum at frequencies less than that of the incident beam. These are the Raman lines. Their separation from the Rayleigh line is a direct measure of the vibrational frequencies of the sample.[1]

The reverse process also occurs. Existing vibrations that have been excited by thermal processes, can be annihilated by coupling with the incident beam and can add their energies to that of the source. These appear as side bands at higher wavenumbers. The Raman process that excites molecular and crystal vibrations is called Stokes scattering; the process that annihilates existing vibrations is called anti-Stokes scattering. The two spectra are mirror images on opposite sides of the Ray-

leigh line (Figure 2). However, because anti-Stokes scattering depends on the existence of thermally activated vibrations, the anti-Stokes intensities are strongly temperature dependent, whereas the Stokes intensities are only weakly temperature dependent. For this reason, anti-Stokes scattering is rarely measured, except for the specialized technique known as *coherent anti-Stokes Raman spectroscopy*.[2] Because the vibrational frequencies are measured by differences between the frequency of the Raman line and the Rayleigh line, most spectrometers are set up to display the difference frequency (wavenumber) directly, defining the exciting frequency as 0. The result sometimes causes confusion: as the displayed Raman wavenumber increases, the true wavenumber decreases. The Raman effect is extremely weak. Rayleigh scattering from optically transparent samples is on the order of 10^{-3}–10^{-5} of the intensity of the exciting line. Raman scattering is from 10^{-3} to 10^{-6} of the intensity of the Rayleigh line. For this reason Raman spectroscopy prior to the 1960s was a highly specialized measurement carried out in a few laboratories mainly with mercury discharge lamp sources, fast prism spectrographs, and photographic plate detectors. In such equipment, the most intense Raman lines are at the threshold of visibility to the darkness-adapted human eye. The invention of continuous gas lasers, which provided the needed intense monochromatic source, and the invention in 1965 of the double monochromator system for stray light discrimination combined to make the modern Raman spectrometer possible.

Instrumentation

Single-Channel Dispersive Instruments

The most widely used equipment for Raman spectroscopy follows the scheme shown in Figure 1. The source is usually a continuous gas laser. The 488-nm and 514.5-nm lines of the argon ion laser are commonly used, although argon has other, somewhat weaker lasing lines that can be used for special purposes. He–Ne lasers (632.8 nm) and the red line of the krypton laser (647.1 nm) also are used. The Raman scattering intensity decreases as the fourth power of the wavelength so that there is an advantage to using the shorter wavelength argon ion lines unless other circumstances, such as sample fluorescence, sample photodecomposition, or the location of the optical absorption edge in semiconductor materials, require a less energetic excitation source. The output from gas lasers is intrinsically polarized so that a polarization rotator is needed to control the polarization orientation with respect to the sample, especially with oriented single-crystal specimens.

The sample holder is indicated by a cube in Figure 1 to show the 90° scattering arrangement. The part of the sample actually measured is a volume, typically 200–500 μm on a side, where the laser beam and the scattered beam intersect. Omitted from the sketch are the focusing optics that collect the scattered light and bring it to a focus on the entrance slit. Many sample mounting arrangements are possible,

depending on the physical state of the sample. An analyzer in front of the entrance slit permits the determination of the polarization of the scattered beam.

The commonly used monochromator is a Czerny–Turner grating type, usually of 1-m focal length, as sketched in Figure 1. This design features two collimating mirrors and a planar grating that is rotated to sweep the spectrum across the exit slit. Because Raman spectra are extremely weak, stray light within the monochromator must be effectively suppressed. The second monochromator, used as a stray light filter, reduces the stray light to the 10^{-12} range, providing a clean background for the Raman spectra.

Photomultipliers are used as detectors in the single-channel instruments. GaAs cathode tubes give a flat frequency response over the visible spectrum to 800 nm in the near IR. Contemporary Raman spectrometers use computers for instrument control, and data collection and storage, and permit versatile displays.

Diode Array and Charge-Coupled Detector Systems

A disadvantage of the single-channel scanning monochromator is that substantial times are needed to collect a spectrum, which is unsatisfactory for transient species, kinetic studies, and observation of unstable compounds. Linear diode array detectors allow the entire spectrum to be captured at one time, although resolution is limited by the number of pixels. Charge-coupled device detector arrays are now used on some commercial spectrometers. These are two-dimensional arrays of detector elements, 578 × 385 pixels being a common choice. Both diode array and charge-coupled detectors permit the use of pulsed laser sources and provide infrared sensitivity. Nd–YAG lasers operating at a wavelength of 1.06 μm can then be used to eliminate many problems of fluorescence and sample photodecomposition.

Fourier Transform Raman Spectrometers

A relatively recent development is the adaptation of Fourier transform spectrometers commonly used for infrared absorption spectroscopy to Raman spectroscopy. Fourier transform Raman spectroscopy has the same advantages as other applications of interferometric techniques. Elimination of the slits greatly increases energy throughput, an important advantage for weak Raman signals. The multiplex advantage permits more rapid accumulation of spectral data, although the alternative of diode array or charge-coupled detectors makes this advantage less important for Raman spectroscopy than for IR spectroscopy.

Sample Requirements

Liquids

Liquids and solutions can be measured in special cells that have optical windows at right angles, or they can be contained in capillary tubes or small vials. The latter are

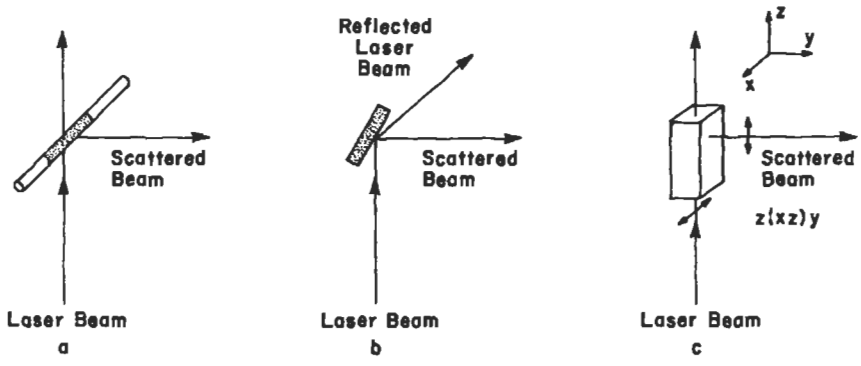

Figure 3 **Scattering geometries appropriate to (a) liquids in capillaries or glass fibers; (b) powder pellets, solid slabs of ceramic or rock, or films on substrates; and (c) oriented single crystals.**

mounted so that the laser passes along one diameter of the capillary while the scattered beam is along a perpendicular diameter (Figure 3).

Powders and Polycrystalline Solids

Usually, particle size has relatively little effect on Raman line shapes unless the particles are extremely small, less than 100 nm. For this reason, high-quality Raman spectra can be obtained from powders and from polycrystalline bulk specimens like ceramics and rocks by simply reflecting the laser beam from the specimen surface. Solid samples can be measured in the 90° scattering geometry by mounting a slab of the solid sample, or a pressed pellet of a powder sample so that the beam reflects from the surface but not into the entrance slit (Figure 3).

Single-Crystal Measurements

Maximum information is obtained by making Raman measurements on oriented, transparent single crystals. The essentials of the experiment are sketched in Figure 3. The crystal is aligned with the crystallographic axes parallel to a laboratory coordinate system defined by the directions of the laser beam and the scattered beam. A useful shorthand for describing the orientational relations (the Porto notation) is illustrated in Figure 3 as $z(xz)y$. The first symbol is the direction of the laser beam; the second symbol is the polarization direction of the laser beam; the third symbol is the polarization direction of the scattered beam; and the fourth symbol is the direction of the scattered beam, all with respect to the laboratory coordinate system.

Spectra From Thick and Thin Films

Raman spectroscopy is especially suited for structural characterization of films and coatings. Both oblique (Figure 3b) and backscattering geometries can be used. The effective penetration depth of the laser depends on film transparency and on the scattering geometry but in most cases the spectrum of the substrate will be superimposed on the spectrum of the film and must be accounted for. The minimum observable film thickness varies with the intrinsic scattering power of the material but is in the range of a few μm for most materials. Resonance enhancement may decrease the minimum thickness. Useful data usually can be obtained from both crystalline and noncrystalline films.

Surface-Enhanced Raman Spectroscopy

Intensity enhancement takes place on rough silver surfaces. Under such conditions, Raman scattering can be measured from monolayers of molecular substances adsorbed on the silver (pyridine was the original test case), a technique known as surface-enhanced Raman spectroscopy.[3] More recently it has been found that surface enhancement also occurs when a thin layer of silver is sputtered onto a solid sample and the Raman scattering is observed through the silver.

High-Temperature and High-Pressure Raman Spectroscopy

Because Raman spectroscopy requires one only to guide a laser beam to the sample and extract a scattered beam, the technique is easily adaptable to measurements as a function of temperature and pressure. High temperatures can be achieved by using a small furnace built into the sample compartment. Low temperatures, easily to 78 K (liquid nitrogen) and with some difficulty to 4.2 K (liquid helium), can be achieved with various commercially available cryostats. Chambers suitable for Raman spectroscopy to pressures of a few hundred MPa can be constructed using sapphire windows for the laser and scattered beams. However, Raman spectroscopy is the characterization tool of choice in diamond-anvil high-pressure cells, which produce pressures well in excess of 100 GPa.[4]

Fluorescence, Sample Heating and Sample Photodecomposition

Although Raman spectroscopy is very versatile with regard to sample form, particle size, and composition, certain interferences occur. Many transparent solid samples contain impurities that fluoresce under excitation by the laser beam. Fluorescence bands are usually extremely broad and are often of sufficient intensity to completely mask the weaker Raman scattering. Fluorescence can sometimes be avoided by using lower energy excitation, such as the red lines of He–Ne or Krypton lasers, or by using a Nd–YAG laser with a diode array detector. If solid samples of interest are being synthesized for measurement, one can sometimes eliminate fluorescence by deliberately doping the sample with luminescence poisons like ferrous iron. Nar-

row-band fluorescence can be distinguished from Raman scattering by measuring the spectra using two different wavelength exciting lines (the 488-nm and 514.5-nm lines of argon, for example). Because the instrument wavenumber scale is set to 0 at the laser line, Raman lines will appear at the same wavenumber position under both excitations whereas fluorescence lines will appear to shift by the wavenumber difference between the two exciting lines.

Because the laser beam is focused on the sample surface the laser power is dissipated in a very small area which may cause sample heating if the sample is absorbing and may cause break-down if the sample is susceptible to photodecomposition. This problem sometimes may be avoided simply by using the minimum laser power needed to observe the spectrum. If that fails, the sample can be mounted on a motor shaft and spun so that the power is dissipated over a larger area. Spinners must be adjusted carefully to avoid defocusing the laser or shifting the focal spot off the optic axis of the monochromator system.

Bulk Raman Spectroscopic Analysis

Fingerprinting

Raman spectra of molecules and crystals are composed of a pattern of relatively sharp lines. The wavenumber scale for most vibrations extends from 50 cm^{-1} to about 1800 cm^{-1} with some molecular vibrations extending to 3500 cm^{-1}. Line widths are on the order of 1–5 cm^{-1}. The Raman spectrum thus has a fairly high density of information and can be used as a fingerprint for the identification of unknown materials by direct comparison of the spectrum of the unknown with spectra in a reference catalog. An example for a series of strontium titanates is shown in Figure 4. This approach is widely used for NMR spectra, X-ray diffraction powder patterns, and infrared spectra as well. As with these other techniques, the success of fingerprinting depends on the availability of a complete, high-quality catalog of reference spectra. Catalogs of reference Raman spectra are much less complete than the corresponding catalogs for IR, ultraviolet, and nuclear magnetic resonance spectra. Users of Raman spectroscopy should compile their own reference spectra.

Crystal Spectra

From a knowledge of the crystal structure it is possible to calculate selection rules for each orientation position and thus gain considerable insight into the vibrational motions of the crystal. The interpretation of such spectra, which show a lot of detail, goes well beyond characterization applications.[5]

Ordered Structures and Phase Transitions

Raman spectroscopy is sensitive to ordering arrangements of crystal structures, the effect depending on the type of order. Ordering atoms onto specific lattice sites in

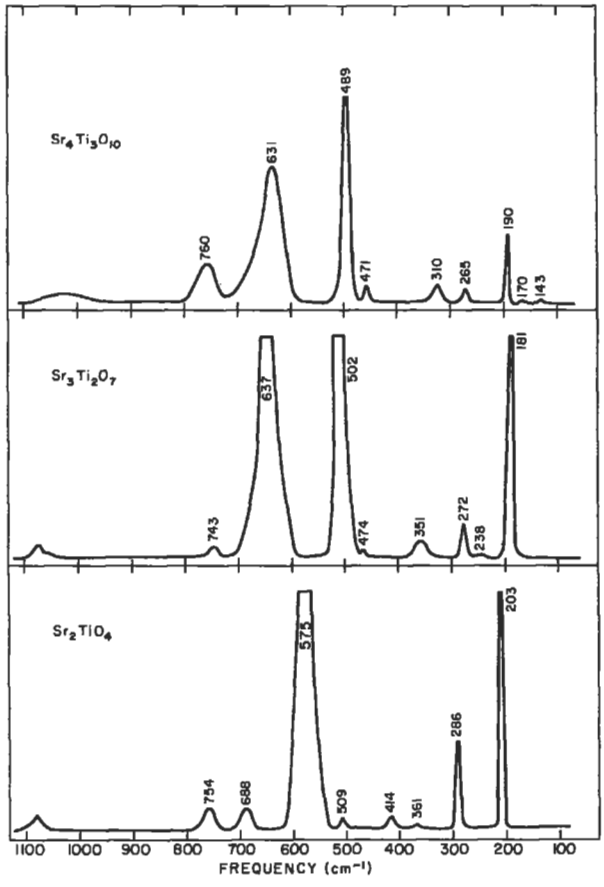

Figure 4 **Raman spectra of a series of strontium titanates showing typical line shapes and information available for fingerprinting. The broadening of the high-wavenumber lines is related to the polar character of the TiO_6 octahedra that occur in all of these structures.**

the parent structure often forms derivative structures having different space groups. The new symmetry leads to relaxed selection rules, which in turn lead to new Raman lines or to the splitting of the lines of the parent structure. Group theoretical calculations allow a good prediction of expected spectral behavior for possible ordering schemes, and Raman (IR) spectra can be used select the correct model.

Some materials undergo transitions from one crystal structure to another as a function of temperature and pressure. Sets of Raman spectra, collected at various temperatures or pressures through the transition often provide useful information on the mechanism of the phase change: first or second order, order/disorder, soft mode, etc.

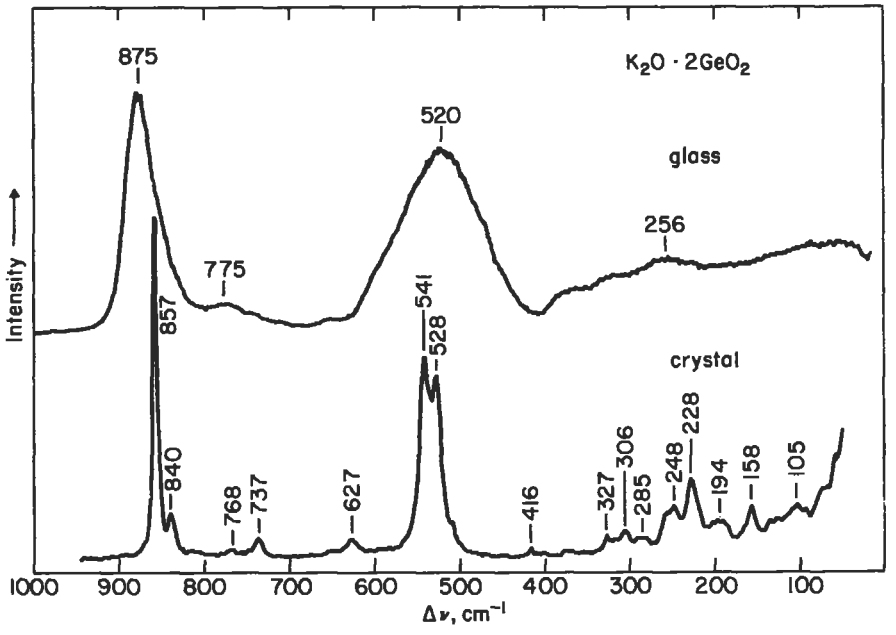

Figure 5 **Raman spectra of crystalline and glassy potassium digermanate showing comparison between crystal spectra and glass spectra.**

Defects and Structural Disorder

Raman spectra of solid solutions, crystals with lattice defects, and systems having other types of structural disorder usually exhibit a pronounced line broadening in comparison with ordered structures. Structural defects, such as lattice vacancies, produce line broadening with little temperature dependence. Orientational disorder, arising from alternative possible orientations of molecules in crystals, dipoles in highly polar crystals, and nonbonding lone pair electrons in ions like Pb^{2+} and As^{3+}, produce Raman lines that are broad at room temperature but become narrow as temperatures are lowered into the liquid nitrogen or liquid helium range. At high defect concentrations, greater than 10–20% mole, the broadened Raman lines give way to a scattering continuum having little structure.

Glasses and Gels

Raman spectroscopy is particularly useful for investigating the structure of noncrystalline solids. The vibrational spectra of noncrystalline solids exhibit broad bands centered at wavenumbers corresponding to the vibrational modes of the corresponding crystals (Figure 5). In silicate glasses shifts in the high-wavenumber bands

is a measure of the degree of polymerization of the silicate network.[6] The processes of nucleation and crystallization in glasses can be readily followed by the Raman spectrum because the sharp crystal bands are easily detected against the much weaker and broader glass bands.

Gels are more disorganized than glasses and often have weaker Raman spectra. The processing steps from solution to sol, to gel, to glass in the sol–gel process of glass making can be followed in the Raman spectra. The loss of organic constituents of the gel can be followed as can the development of the bulk glass structure.

Microfocus Raman Spectroscopic Analysis

By successfully marrying a Raman spectrometer to an optical microscope it is possible to obtain spectra having the resolution of optical microscopy—a few μm. The essential feature is a beam splitter through which the laser beam passes on its way to the microscope objective. The beam emerges from the objective to strike a sample held on a standard microscope stage. Raman scattering is observed in the backscattering geometry. The scattered beam also passes through the beam splitter and reaches the entrance slit of the monochromator.

Grain-by-Grain Analysis and Crystal Zoning

The obvious application of microfocus Raman spectroscopy is the measurement of individual grains, inclusions, and grain boundary regions in polycrystalline materials. No special surface preparation is needed. Data can be obtained from fresh fracture surfaces, cut and polished surfaces, or natural surfaces. It is also possible to investigate growth zones and phase separated regions if these occur at a scale larger than the 1–2 μm optical focus limitation.

With a special optical system at the sample chamber, combined with an imaging system at the detector end, it is possible to construct two-dimensional images of the sample displayed in the emission of a selected Raman line.[7] By imaging from their characteristic Raman lines, it is possible to map individual phases in the multiphase sample; however, Raman images, unlike SEM and electron microprobe images, have not proved sufficiently useful to justify the substantial cost of imaging optical systems.

Precipitates and the Liquid/Solid Interface

With the microfocus instrument it is possible to combine the weak Raman scattering of liquid water with a water-immersion lens on the microscope and to determine spectra on precipitates in equilibrium with the mother liquor. Unique among characterization tools, Raman spectroscopy will give structural information on solids that are otherwise unstable when removed from their solutions.

Fluid Inclusions

Natural crystals, synthetic crystals, and glasses often contain small bubbles that preserve samples of the fluid from which the crystals grew or of the atmosphere over the glass melt. Using a long focal length lens, the laser beam can be focused into inclusions at some depth below the crystal or glass surface. The Raman spectra then permit the identification of molecular species dissolved in the aqueous solutions or of components in the gas bubbles.[8]

Grain Boundaries, Cracks, and Stressed Materials

Stress in crystalline solids produces small shifts, typically a few wavenumbers, in the Raman lines that sometimes are accompanied by a small amount of line broadening. Measurement of a series of Raman spectra in high-pressure equipment under static or uniaxial pressure allows the line shifts to be calibrated in terms of stress level. This information can be used to characterize built-in stress in thin films, along grain boundaries, and in thermally stressed materials. Microfocus spectra can be obtained from crack tips in ceramic material; and by a careful spatial mapping along and across the crack estimates can be obtained of the stress fields around the crack.[9]

Thick and Thin Films

Because it is nondestructive, can be fine focused, and can be used in a backscattering geometry, Raman spectroscopy is a useful tool for characterizing films and layers either free standing or on various substrates. Semiconductors such as silicon, germanium and GaAs produce Raman spectra that give information on film crystallinity, the presence of impurity layers, and the presence of amorphous material. Films are ideal samples on the microscope stage of the microfocus instrument, and comparisons can easily be made between centers and margins of deposition zones. Raman spectroscopy has been applied to the characterization of chemical vapor deposition-grown diamond films, proving the formation of diamond and characterizing the presence of graphite and various amorphous carbons.[10]

The depth of film penetrated and sampled depends on the transparency of the sample to the laser radiation used. This is strongly dependent on the sample material and on the laser wavelength, and can vary from as little as a few μm to significant fractions of a mm. If a film or coating is transparent, the film/substrate interface and any other material deposited there is also accessible and may provide a detectable Raman signal. The absolute sensitivity of the Raman technique is routinely such that a film thickness of at least 0.1 μm is required to provide a workable signal. Special instrumentation, particularly high-sensitivity detectors, can reduce this to a few tens of nm and, as mentioned already, for surface-enhanced Raman scattering of molecules adsorbed on rough silver (and a few other) surfaces, submonolayer amounts are detectable.

Conclusions

Raman spectroscopy is a very convenient technique for the identification of crystalline or molecular phases, for obtaining structural information on noncrystalline solids, for identifying molecular species in aqueous solutions, and for characterizing solid–liquid interfaces. Backscattering geometries, especially with microfocus instruments, allow films, coatings, and surfaces to be easily measured. Ambient atmospheres can be used and no special sample preparation is needed.

In-situ Raman measurements will become more important in the future. In many types of vapor and liquid deposition systems, it is important to monitor the progress of reactions and changes in structure as films or crystals are grown. Fiber optic cables, sapphire light pipes and other optical systems are available for bringing the laser beam into the reaction chamber and for collecting the scattered light. Spectra can be collected without disturbing the deposition process.

Related Articles in the Encyclopedia

FTIR and HREELS

References

1 D. A. Long. *Raman Spectroscopy.* McGraw-Hill, New York, 1977. A standard reference work on Raman spectroscopy with much theoretical detail on the underlying physics. Most of the needed equations for any application of Raman spectroscopy can be found in this book.

2 W. M. Tolles, J. W. Nibler, J. R. McDonald, and A. B. Harvey. *Appl. Spectros.* **31,** 253, 1977.

3 R. K. Chang and T. E. Furtak. *Surface Enhanced Raman Scattering.* Plenum, New York, 1982. A collection of individually authored papers describing many different applications of SERS.

4 R. J. Hemley, P. M. Bell, and H. K. Mao. *Science.* **237,** 605, 1987.

5 G. Turrell. *Infrared and Raman Spectra of Crystals.* Academic, London, 1972. One of the best available texts describing the principles of Raman scattering from crystals. Includes factor group calculations, polarization measurements, force constant calculations, and many other aspects of crystal physics.

6 B. O. Mysen, D. Virgo, and F. A. Seifert. *Rev. Geophys. Space Phys.* **20,** 353, 1982.

7 P. Dhamelincourt, F. Wallart, M. Leclercq, A. T. N'Guyen, and D. O. Landon. *Analyt. Chem.* **51,** 414A, 1979.

8 J. D. Pasteris, B. Wopenka, and J. C. Seitz. *Geochim. Cosmochim. Acta.* **52,** 979, 1988.

9 R. H. Dauskardt, D. K. Veirs, and R. O. Ritchie. *J. Amer. Ceram.* Soc. 72, 1124, 1989.

10 D. S. Knight and W. B. White. *J. Mat. Res.* **4,** 385, 1989.

8.3 HREELS

High-Resolution Electron Energy Loss Spectroscopy

BRUCE E. KOEL

Contents

Introduction

High-resolution electron energy loss spectroscopy (HREELS) has emerged over the past decade as a sensitive, versatile, nondestructive surface analysis technique used to study the vibrations of atoms and molecules in and on solid surfaces.[1-4] Energy loss peaks in the spectra correspond to vibrations of atoms in the surface layers of a solid or in adsorbed molecules. The principal analytical use is to detect the presence of molecular groups on surfaces, often submonolayer amounts of adsorbed species, by observation of their vibrational spectra, and to chemically identify what these species are from the details (positions and intensities) of the vibrational peaks. For molecular materials, such as polymers, such information may be obtained also about the surface of the solid itself. The information obtained is of the same kind as that in infrared and Raman spectroscopy. The main reasons for the popularity of HREELS over these optical methods are its very small detection limit and its wide spectral range at high surface sensitivity. Most HREELS studies are of single-crystal surfaces, however polycrystalline and noncrystalline samples also can be studied with this technique, but with reduced effectiveness.

Fundamental information from vibrational spectra is important for understanding a wide range of chemical and physical properties of surfaces, e.g., chemical reactivity and forces involved in the atomic rearrangement (relaxation and reconstruction) of solid surfaces. Practical applications of HREELS include studies of:

1 Functional groups on polymer and polymer film surfaces
2 Phonon modes of metals and films, semiconductors, and insulators
3 Concentrations of free charge carriers in semiconductors
4 Adsorbed species (and even underlayer atoms) on single-crystal surfaces
5 Kinetics of surface processes when used in a time-resolved mode.

Of these, the most extensive use is to identify adsorbed molecules and molecular intermediates on metal single-crystal surfaces. On these well-defined surfaces, a wealth of information can be gained about adlayers, including the nature of the surface chemical bond, molecular structural determination and geometrical orientation, evidence for surface-site specificity, and lateral (adsorbate–adsorbate) interactions. Adsorption and reaction processes in model studies relevant to heterogeneous catalysis, materials science, electrochemistry, and microelectronics device failure and fabrication have been studied by this technique.

The first vibrational spectrum of adsorbed molecules obtained by inelastic scattering of low energy electrons was obtained by Propst and Piper in 1967. Over the next ten years, Ibach in Jülich achieved much higher resolution and, along with several other research groups, developed and used the new technique (HREELS) to study a wide range of surface vibrations, including polyatomic molecules adsorbed on surfaces. The enthusiasm existed mainly because HREELS could be used to study adsorbates on low surface-area, opaque, metal single-crystal samples, something that could not be done with infrared and Raman spectroscopy. It is now well-established as an important vibrational spectroscopy at surfaces, and its utility as an analytical tool with extreme surface sensitivity is rapidly being extended.

Basic Principles

Electron Scattering

At sufficiently high resolution, quasi-elastically scattered electrons have an inelastic scattering distribution from exciting surface vibrational modes such as surface phonons and adsorbate vibrations. (See, for example, Figure 1, the case of CO adsorbed on a Rh surface.) These modes have excitation energies below 0.5 eV (4000 cm^{-1}). The basis of the kinematic (single scattering) description of electron scattering from surfaces is conservation of energy and momentum parallel to the surface. These conservation laws define the scattering possibilities and, along with the vibrational energies, determine the peak energies in HREELS. The mechanisms

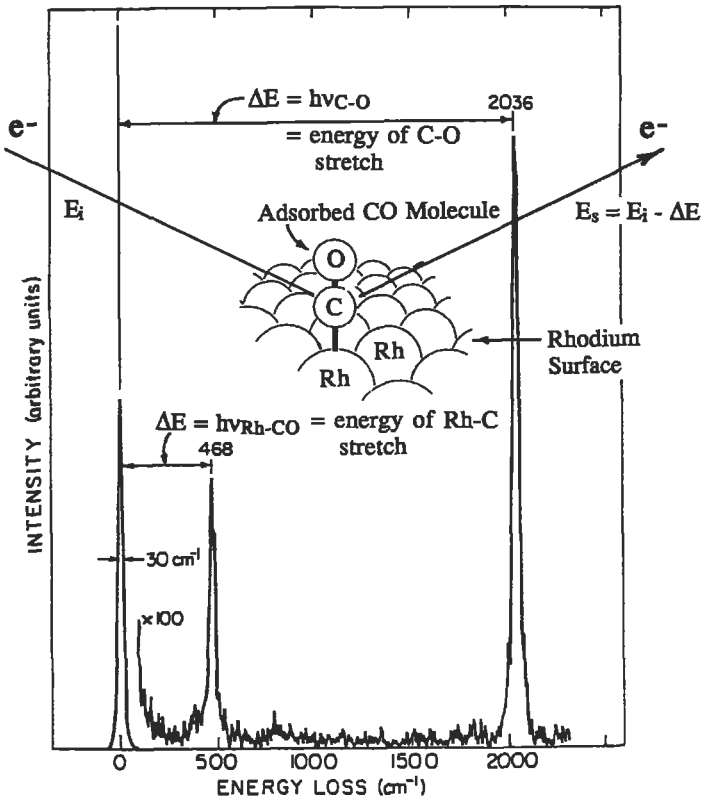

Figure 1 **Schematic of electron energy-loss scattering process for electrons of energy E_i striking a Rh single-crystal surface with adsorbed CO molecules present. The actual energy-loss spectrum, due to excitation of CO vibrations, is shown also.**

of electron inelastic scattering determine the scattering cross sections (probabilities), and therefore the intensities of vibrational energy loss peaks.

Two different electron inelastic scattering mechanisms are most important for explaining the intensities and angular distribution of peaks observed in HREELS: dipole and impact scattering. Dipole scattering is due to the long-range part of the electrostatic interaction between an incoming electron and the dipolar electric field of the vibrating (oscillating) atoms at the surface. Energy exchange takes place at a long distance (50 Å) from the surface. This leads to small angle scattering and so the scattered intensity is strongly peaked near the specular direction, with a half-angle $\Delta\theta \sim 0.1$–$1°$. The dominance of this mechanism for detection at the specular direction leads to the dipole selection rule in HREELS, that is identical to that associated with reflection infrared spectroscopy: Only vibrational modes which produce a

dynamic (oscillating) dipole moment perpendicular to the metal surface are dipole-active, i.e., will produce energy loss peaks on-specular. The origin of this selection rule is the screening of a charge on a conducting surface by an image charge induced in the free electrons. Dynamic dipoles parallel to the surface generate no long-range dipole field, while dynamic dipoles perpendicular to the surface generate a long-range dipole field that is enhanced by a factor of 2.

At large scattering angles away from the specular direction, one enters the impact scattering regime. This mechanism is due to a short range electrostatic interaction between an incoming electron and the ion cores of the adsorbate and substrate lattice. Impact scattering is usually several orders of magnitude weaker than dipole scattering at the specular direction in the low-energy regime (below 10 eV). Broad angular scattering distributions having intensities proportional to vibrational amplitudes are characteristic. Selection rules are much less restrictive and are based on adsorbate site symmetry and vibrational mode polarization in relation to the scattering plane of incidence. The impact scattering regime extends to several hundred eV, and the theory of these interactions must include multiple scattering. Measurements of inelastic scattering cross sections in this regime have a great potential for structural analysis, but have been made experimentally only recently.

A type of molecular resonance scattering can also occur from the formation of short-lived negative ions due to electron capture by molecules on surfaces. While this is frequently observed for molecules in the gas phase, it is not so important for chemisorbed molecules on metal surfaces because of extremely rapid quenching (electron transfer to the substrate) of the negative ion. Observations have been made for this scattering mechanism in several chemisorbed systems and in physisorbed layers, with the effects usually observed as small deviations of the cross section for inelastic scattering from that predicted from dipole scattering theory.

While the underlying mechanisms of HREELS are pretty well understood, many important details relating to selection rules and scattering cross sections remain unknown.

Vibrations at Surfaces

Vibrations give molecular information by identifying which atoms are chemically bonded together. The frequency of a vibrational mode is related to the bond force constant and reduced mass of the vibrating atoms. Reasonable correlations exist between the number of bonds, bond energy, and force constant for vibrations within molecular species at surfaces and for adsorbate–substrate vibrations. It would be extremely useful if one could determine chemical bond strengths from vibrational spectra, but the accurate determination of this quantity is quite ambiguous. Frequency shifts occur as the concentration is changed in adsorbed layers as a result of local bonding variations due to changing sites or bond energies, dipole–dipole coupling leading to collective vibrations of the overlayer, or other factors.

The intensity of a vibrational mode in HREELS on-specular is given by the ratio of the inelastic to elastic intensities

$$S = 4\pi E_i^{-1} N P_p^2 F(\alpha, \theta) \arccos\theta \tag{1}$$

where S is the dipole scattering cross section, E_i is the primary beam energy, N is the number of surface oscillators, P_p is the perpendicular component of the dynamic dipole moment, and $F(\alpha, \theta)$ is an instrument and geometry factor. This intensity (sensitivity) can be optimized by considering the detected inelastic current, I:

$$I = I_0 R(E_i) KS \tag{2}$$

where I_0 is the incident beam current, $R(E_i)$ is the metal surface reflectivity (typically 1–10%) for the primary beam energy E_i, and K is the analyzer transmission constant. The function S is a smoothly decreasing function of energy and is proportional to E_i^{-1} for a layer of adsorbed dipoles, but R exhibits significant variation as a function of E_i. Operationally, the incident energy is tuned to give an intense elastic peak at a low energy (< 10 eV) where S is large.

The sensitivity of HREELS is largest for molecules, materials, or particular vibrations, that have large S. Normalizing for the other variables, such as concentration, leads to a general rule that vibrational modes that are observed as strong bands in infrared spectroscopy of gases or of condensed phases will give rise to intense loss peaks in HREELS. For example, carbonyl (C = O) stretching modes have larger intensities than hydrocarbon C–H stretching modes in IR of bulk phases and also in HREELS on surfaces. Orientational effects will affect this sensitivity in accord with the dipole selection rule.

Quantitative analysis and determination of the concentration of surface species requires measuring peak intensities and accounting for vibrational cross sections. This is a difficult task. Careful analysis of K and analyzer angular characteristics is required when determining $S(E_i)$. To obtain information on the charges on atoms at the surface, one could perform a calculation of dynamic dipole moments (or effective charges) from knowledge of S, in principle. In practice, one usually assumes a point dipole model and gas phase polarizabilities for surface species, and this has lead to anomalously low values in the case of adsorbed molecules on metals. Chemical bonding effects greatly enhance the electronic polarizability of chemisorbed molecules and enhance the dielectric screening by the adlayer, reducing the predicted vibrational (inelastic peak) intensity.

The width and shape of the energy loss peaks in HREELS are usually completely determined by the relatively poor instrumental resolution. This means that no information can be obtained from HREELS about such interesting chemical physics questions as vibrational energy transfer, since the influence of the time scale and mechanism of vibrational excitations at surfaces on the lifetimes, and therefore the line widths and shapes, is swamped. (Adsorbates on surfaces have intrinsic vibra-

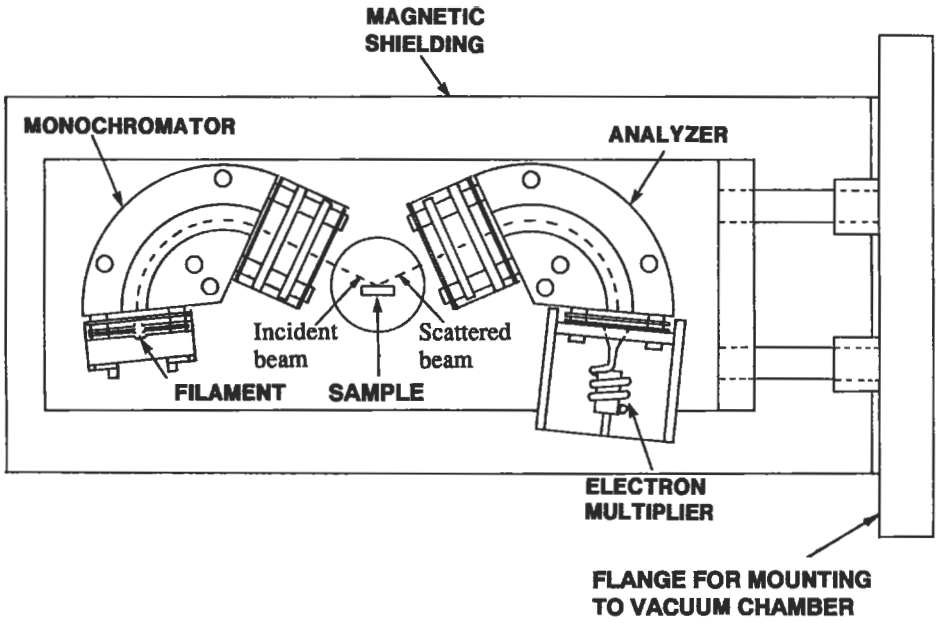

Figure 2 **Schematic of a 127° high-resolution electron energy-loss spectrometer mounted on an 8-in flange for studies of vibrations at surfaces.**

tional line widths of typically 5 cm^{-1} (0.6 meV) and Lorentzian line shapes.) A practical matter is that this poor resolution is insufficient to resolve closely overlapping vibrational frequencies.

Instrumentation

In HREELS, a monoenergetic beam of low energy electrons is focused onto the sample surface and the scattered electrons are analyzed with high resolution of the scattering energy (< 10 meV or 80 cm^{-1}) and angle ($\Delta\theta$ = 2–5°). This is achieved by using electrostatic spectrometers, typically with 127° cylindrical dispersive elements. Hemispherical and cylindrical mirror analyzers have been used also. Some typical analyzer parameters are 25-mm mean radius, 0.1-mm slit width, and 0.5-eV pass energies. Refinements also include the addition of tandem cylindrical sectors to the monochromator and analyzer. A number of commercial versions of spectrometers are capable of routine and dependable operation.

A simple spectrometer that we have used successfully is shown in Figure 2. Electrons from an electron microscope hairpin tungsten filament are focused with an Einzel lens onto the monochromator entrance slit, pass through the monochromator and exit slit, and are focused on the sample's surface by additional electrostatic

lenses (in this case a double plate lens system). The incident beam energy is usually below 10 eV, where dipole scattering cross sections are strong, and the beam current to the sample is typically 0.1–1 nA. Electrons that are reflected from the sample's surface are focused on the analyzer entrance slit and energy analyzed to produce an electron energy loss (vibrational) spectrum. An electron multiplier and pulse counting electronics are used due to the small signals. Count rates in HREELS are typically 10^4–10^6 counts/sec for elastically scattered electrons and 10–10^3 counts/sec for inelastically scattered electrons. Scan times typically range from about five minutes to several hours.

The exact incident and scattering angles (~ 60° from the surface normal) are not critical, but a specular scattering geometry must be attainable. It is also very useful to be able to observe a nonspecular scattering angle either by rotating the crystal about an axis perpendicular to the scattering plane or by rotating one of the analyzers in the scattering plane. Magnetic shielding must surround the spectrometer because the magnetic field of the earth and any nearby ion pumps will distort the trajectories of the electrons within the spectrometer, because of their small kinetic energies. The spectrometer is mounted in a ultrahigh-vacuum chamber and analysis must be carried out at pressures below 10^{-4} torr. This requirement exists because of the sensitivity of the electron filament and slits to reactions with background gases. Higher pressure gas phase molecules also will cause inelastic scattering that obscures the surface spectra. The applicability of the HREELS technique can be greatly extended by combining it with a high-pressure reaction chamber and sample transfer mechanism. We have previously used this type of system to study hydrogen transfer in adsorbed hydrocarbon monolayers at atmospheric pressure.

Interpretation of Vibrational Spectra

In the following discussion, heavy emphasis is made of examples from studies of adsorbed layers on metal single-crystal samples. These illustrate the power of the HREELS technique and represent the main use of HREELS historically. Certainly HREELS has been used outside of the single-crystal world, and mention is made concerning its use on "practical" materials. This latter use of HREELS represents a true frontier.

Identification of Adsorbed Species

Determination of surface functional groups, e.g., –OH, –C ≡ C–, and >C = O, and identification of adsorbed molecules comes principally from comparison with vibrational spectra (infrared and Raman) of known molecules and compounds. Quick qualitative analysis is possible, e.g., stretching modes involving H appear for ν(C–H) at 3000 cm^{-1} and for ν(O–H) at 3400 cm^{-1}. In addition, the vibrational energy indicates the chemical state of the atoms involved, e.g., ν(C=C) ~ 1500 cm^{-1} and ν(C=O) ~ 1800 cm^{-1}. Further details concerning the structure of adsorbates

Mode assignment	$CH_3CCo_3(CO)_9$ [6]	CH_3C–Rh (111) [5]
$\nu_{as}(CH_3)/\nu_{as}(CD_3)$	2930 (m)/2192 (w) e	2920 (vw)/2178 (vw) e
$\nu_s(CH_3)/\nu_s(CD_3)$	2888 (m)/— a_1	2880 (w)/2065 (vw) a_1
$\delta_{as}(CH_3)/\delta_{as}(CD_3)$	1420 (m)/1031 (w) e	1420 (vw)/— e
$\delta_s(CH_3)/\delta_s(CD_3)$	1356 (m)/1002 (vw) a_1	1337 (s)/988 (w) a_1
ν(CC)	1163 (m)/1882 (ms) a_1	1121 (m)/1145 (m) a_1
$\rho(CH_3)/\rho(CD_3)$	1004 (s)/828 (s) e	972 (vw)/769 (vw) e
ν_s(M–C)	401 (m)/393 (m) a_1	435 (w)/419 (w) a_1

* Intensities of the spectral bands are given in parentheses following the band frequencies using the following abbreviations: vs = very strong, s = strong, ms = medium strong, m = medium, w = weak, and vw = very weak. Symmetry assignments for each of the vibrational modes are also indicated after the band frequencies.

Table 1 **Comparison of the vibrational frequencies (cm^{-1}) of the ethylidyne surface species formed on Rh (111) with those of the ethylidyne cluster compound.***

comes from comparison to vibrational spectra of ligands in metal cluster compounds whose X-ray crystal structure is known. Isotopic substitution is extremely important in confirming vibrational assignments. Only H/D substitution can be carried out, due to the low resolution, but this is useful for an enormous range of adsorbed molecules, including hydrocarbons. Substituting D for H causes an isotopic shift of $\sqrt{2}$ for those modes with large-amplitude H motion.

As an example, Figure 3a shows the HREELS spectra after the adsorption of ethylene ($H_2C = CH_2$) on Rh(111) at 310 K.[5] Comparison with gas phase ethylene infrared spectra shows that large changes occurred during adsorption, e.g., ν(C–H) = 2880 cm^{-1}, indicative of aliphatic C–C–H bonds, rather than the expected ν(C-H) ~ 3000 cm^{-1} for olefinic C=C–H bonds. The complete agreement with frequencies, intensities, and H/D shifts observed in IR spectra (and normal mode analysis) of an organometallic complex, $CH_3CCo(CO)_9$,[6] allowed for the detailed assignment of the loss peaks to vibrational modes of a surface ethylidyne (CCH_3) species, as shown in Figure 3b and Table 1.

The lack of a well-defined specular direction for polycrystalline metal samples decreases the signal levels by 10^2 –10^3, and restricts the symmetry information on adsorbates, but many studies using these substrates have proven useful for identifying adsorbates. Charging, beam broadening, and the high probability for excitation of phonon modes of the substrate relative to modes of the adsorbate make it more difficult to carry out adsorption studies on nonmetallic materials. But, this has been done previously for a number of metal oxides and compounds, and also semicon-

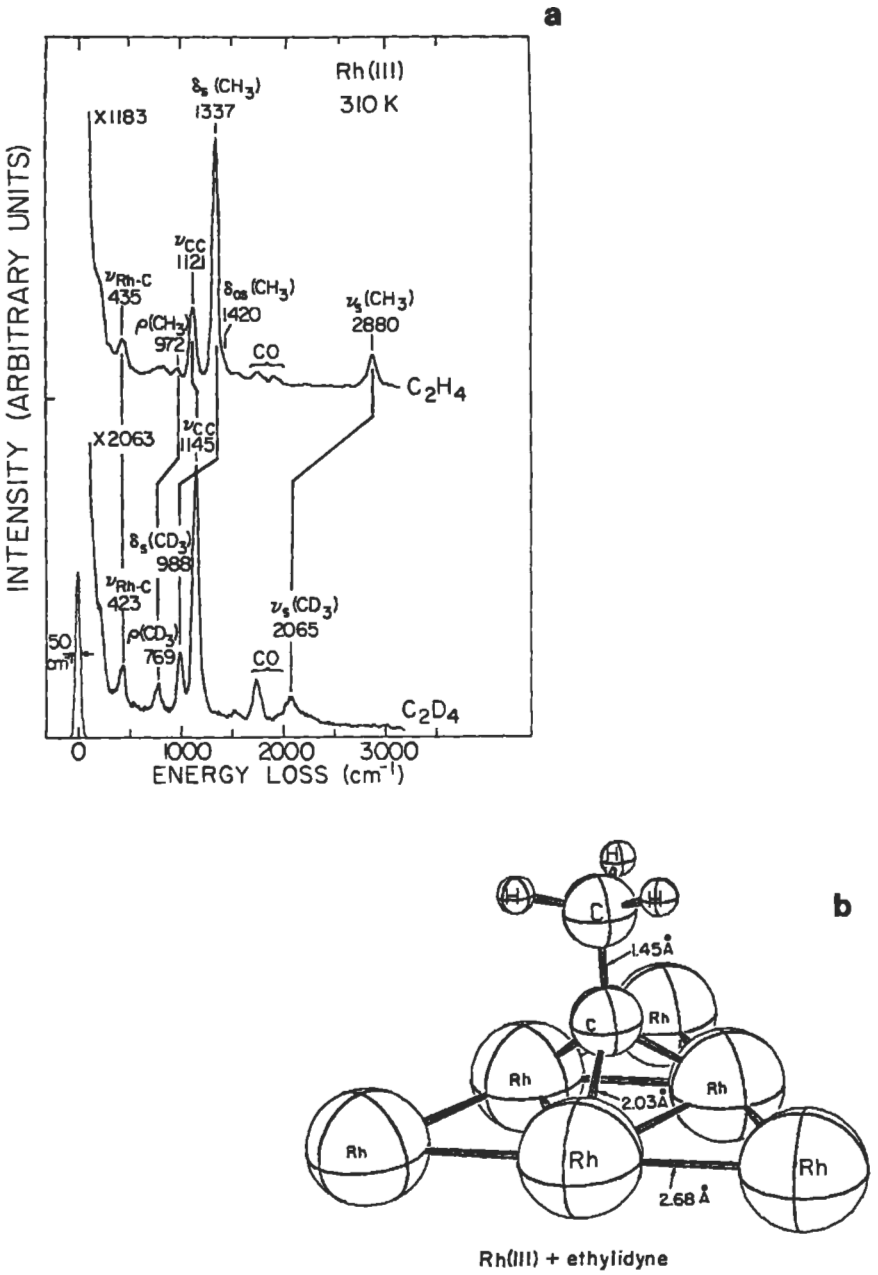

Figure 3 **(a) Specular spectra in HREELS obtained following exposure of ethylene (C_2H_4 or C_2D_4) on Rh(111) at 310 K to form the ethylidyne (CCH_3) surface species.[2] (b) The atomic structure (bond distances and angles) of ethylidyne as determined by LEED crystallography.**

ductors like Si, InP, and diamond. Dubois, Hansma, and Somorjai fabricated model supported metal catalysts by evaporating rhodium onto an oxidized aluminum substrate and studied CO adsorption by using HREELS. We also have used HREELS to characterize lubricating carbon films on small samples of actual magnetic recording disk heads.

Determination of Adsorption Geometry

The symmetry of an adsorbed molecule and its orientation relative to the surface plane can be established using group theory and the dipole selection rule for specular scattering. The angular variations of loss intensities determines the number and frequencies of the dipole active modes. Only those modes that belong to the totally symmetric representations of the point group which describes the symmetry of the adsorbed complex will be observed as fundamentals on-specular. The symmetry of the adsorbate-surface complex is then determined by comparing the intensity, number, and frequency of dipole-active modes with the correlation table of the point group of the gas phase molecule. In the previous example of adsorbed ethylidyne, observation of an intense symmetric C–H bending ($\delta_s CH_3$) loss peak and weak antisymmetric C–H bending ($\delta_{as} CH_3$) loss peak establishes C_{3v} symmetry for the surface complex.

The adsorption of nitrogen dioxide (NO_2) on metal surfaces is a beautiful example of linkage isomerism, as illustrated in Figure 4, that was discovered by using HREELS.[7] Gas phase NO_2 has C_{2v} symmetry which is retained in the top two binding geometries (Figures 4b and c) since the asymmetric ONO stretching (ν_{as}) is not observed on-specular. The symmetry is reduced to C_s when NO_2 is bonded as the bridging isomer (Figure 4a) and ν_{as} is dipole-active. Confirmation of these bonding geometries (and the correct assignment of the two C_{2v} isomers) comes from comparison with transition metal complexes containing the nitrite (NO_2^-) ligand.

Determination of Adsorption Site

While there is a general pattern of decreased metal-atom stretching frequency with increasing coordination of the adsorption site for the same metal–adatom combination, no site assignments can be made simply by observing the vibrational frequency. Surface chemical bonds clearly control the site dependent vibrational shifts of adsorbed species. Detailed studies that often involve impact scattering can determine the adatom adsorption site in some cases. For polyatomic molecules, bonding to one or more metal atoms at the surface can not be distinguished in general. Good correlation does exist between the C–O stretching frequency (ν_{CO}) for adsorbed CO and the adsorption site: $\nu_{CO} > 2000$ cm^{-1} indicates an *atop* site (bonding to a single metal atom); 1850 cm^{-1} $> \nu_{CO} >$ 2000 cm^{-1} indicates a *bridge* site (bonding to two metal atoms); and $\nu_{CO} <$ 1850 cm^{-1} indicates a threefold or fourfold bridge site (bonding in a region between three or four metal atoms). This correlation has

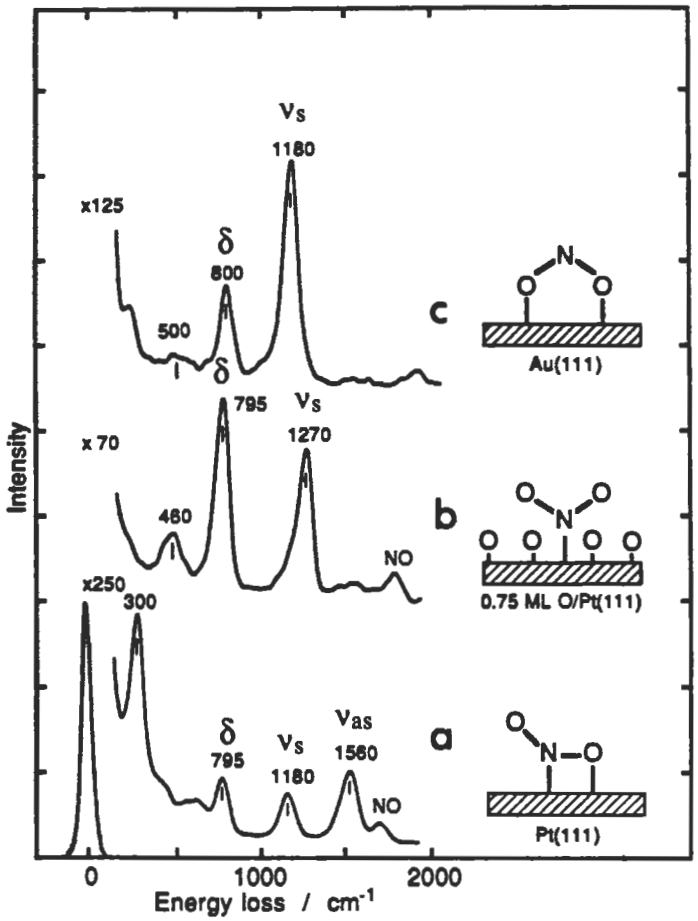

Figure 4 **Specular spectra in HREELS of NO_2 adsorbed in three different bonding geometries.[7]**

been established by measuring the vibrational spectrum in conjunction with determining the adsorption site for CO by LEED crystallography calculations, and also by examining the correlations for CO bonded in organometallic clusters. Similar correlations are likely to exist for other diatomic molecules bonded to surfaces, e.g., NO, based on correlations observed in organometallic clusters but this has not been investigated sufficiently.

Figure 5 shows the utility of HREELS in establishing the presence of both bridge-bonded and atop CO chemisorbed on Pt(111) and two SnPt alloy surfaces, and also serves to emphasize that HREELS is very useful in studies of metal alloys.[8] The ν_{CO} peaks for CO bonded in bridge sites appear at 1865, 1790, and 1845 cm^{-1} on the Pt(111), (2×2) and $\sqrt{3}$ surfaces, respectively. The ν_{CO} peaks for CO

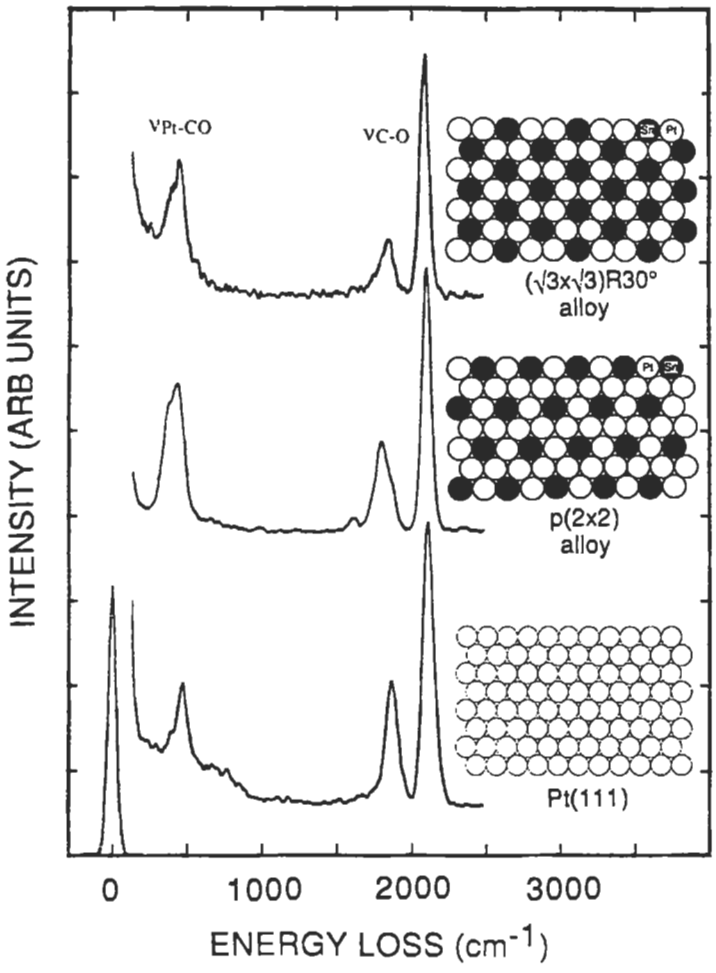

Figure 5 **HREELS of the saturation coverage of CO on Pt(111) and the (2 × 2) and ($\sqrt{3} \times \sqrt{3}$) R30° Sn/Pt surface alloys.[8]**

bonded in atop sites appear at 2105, 2090, and 2085 cm^{-1} on the Pt(111), (2 × 2) and $\sqrt{3}$ surfaces, respectively. Also, lower frequency $\nu_{Pt\text{-}CO}$ peaks accompany each of the ν_{CO} peaks. As discussed previously, the peak intensities are not necessarily proportional to the concentration of each type of CO species and the exact ν_{CO} frequency is determined by many factors.

Other Applications

Many other surfaces can be investigated by HREELS. As larger molecule and non-single-crystal examples, we briefly describe the use of HREELS in studies of polymer surfaces. The usefulness of HREELS specifically in polymer surface science

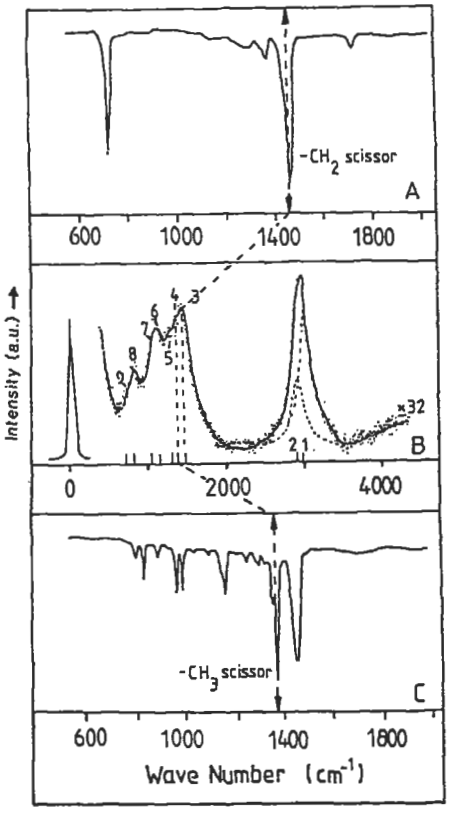

Figure 6 **Vibrational spectra of polymers. (a) Transmission infrared spectrum of polyethylene; (b) electron-induced loss spectrum of polyethylene; (c) transmission infrared spectrum of polypropylene.[10]**

applications has recently been reviewed by Gardella and Pireaux.[9] HREELS is absolutely nondestructive and can be used to obtain information on the chemical composition, morphology, structure, and phonon modes of the solid surface.

Many polymer surfaces have been studied, including simple materials like polyethylene, model compounds like Langmuir-Blodgett layers, and more complex systems like polymer physical mixtures. Figure 6 shows an HREELS spectrum from polyethylene [CH_3–$(CH_2)_n$–CH_3]. Assignment of the energy loss peaks to vibrational modes is done exactly as described for adsorbates in the preceding section. One observes a peak in the C–H stretching region near 2950 cm^{-1}, along with peaks due to C–C stretching and bending and C–H bending modes in the "fingerprint" region between 700–1500 cm^{-1} from both the –CH_3 (which terminate the chains) and –CH_2– groups in the polymer. Since the CH_3/CH_2 ratio is vanishingly small in the bulk of the polymer, the high intensity of the –CH_3 modes indicate

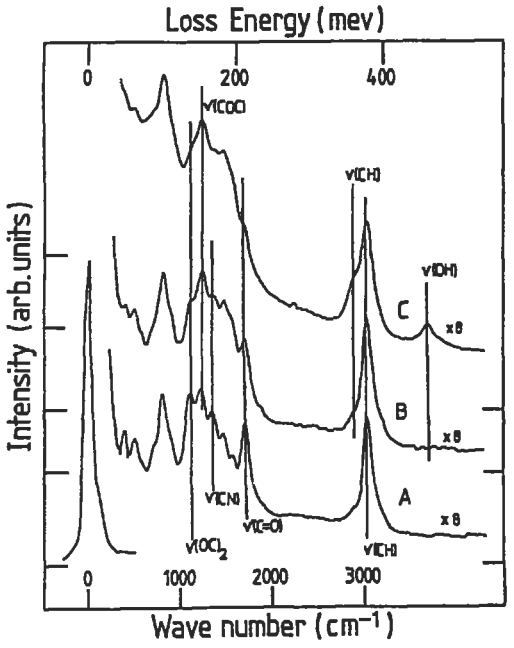

Figure 7 **HREELS vibrational spectra of the interface formation between a polyimide film and evaporated aluminum: (a) clean polyimide surface; (b) with 1/10 layer of Al; (c) with1/2 layer of Al.[11]**

that they are located preferentially in the extreme outer layers of the polymer surface.[10]

HREELS is useful in many interfacial problems requiring monolayer sensitivity. The incipient formation of the interface between a clean cured polyimide film and deposited aluminum has been studied using HREELS,[11] as shown in Figure 7. The film was PMDA-ODA [poly-N,N'–bis(phenoxyphenyl)pyromellitimide], shown schematically in Figure 8. At low Al coverage, the ν(C=O) peak at 1720 cm^{-1} is affected strongly, which indicates that Al reacts close to the carbonyl site. At higher Al coverage, new peaks at ~ 2950 and 3730 cm^{-1} appear which are due to aliphatic $-CH_x$ and –OH groups on the surface. This is evidence for bond scissions in the polymer skeleton.

In general, the main problems with the analysis of bulk polymers has been charging and rough surfaces. The latter characteristic makes the specular direction poorly defined, which causes diffuse and weak electron scattering. Preparation of the polymer as a thin film on a conducting substrate can overcome the charging problem. Even thick samples of insulating polymers can now be studied using a "flood gun" technique. Thiry and his coworkers[12] have shown that charging effects can be over-

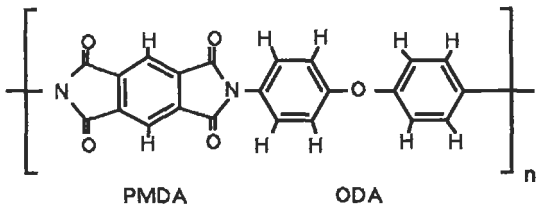

Figure 8 **Structure of PMDA–ODA.**

come by using an auxiliary defocused beam of high-energy electrons to give neutralization of even wide-gap insulators, including Al_2O_3, MgO, SiO_2, LiF, and NaCl.

Comparison to Other Techniques

Information on vibrations at surfaces is complementary to that provided on the compositional analysis by AES and SIMS, geometrical structure by LEED, and electronic structure by XPS and UPS. Vibrational spectroscopy is the most powerful method for the identification of molecular groups at surfaces, giving information directly about which atoms are chemically bonded together. These spectra are more directly interpreted to give chemical bonding information and are more sensitive to the chemical state of surface atoms than those in UPS or XPS. For example, the C(1s) binding energy shift in XPS between C=O and C–O species is 1.5 eV and that between C=C and C–C species is 0.7 eV, with an instrumental resolution of typically 1 eV. In contrast, the vibrational energy difference between C=O and C–O species is 1000 cm^{-1} and that between C=C and C–C species is 500 cm^{-1}, with an instrumental resolution of typically 60 cm^{-1}. Vibrational spectroscopy can handle the complications introduced by mixtures of many different surface species much better than UPS or XPS.

Many other techniques are capable of obtaining vibrational spectra of adsorbed species: infrared transmission-absorption (IR) and infrared reflection-absorption spectroscopy (IRAS), surface enhanced Raman spectroscopy (SERS), inelastic electron tunneling spectroscopy (IETS), neutron inelastic scattering (NIS), photoacoustic spectroscopy (PAS), and atom inelastic scattering (AIS). The analytical characteristics of these methods have been compared in several reviews previously. The principle reasons for the extensive use of the optical probes, e.g., IR, compared to HREELS in very practical nonsingle-crystal work are the higher resolution (0.2–8 cm^{-1}) and the possibility for use at ambient pressures. HREELS could be effectively used to provide high surface sensitivity and a much smaller sampling depth (< 2 nm) and wider spectral range (50–4000 cm^{-1}) than many of these other methods.

HREELS is used extensively in adsorption studies on metal single crystals, since its high sensitivity to small dynamic dipoles, such as those of C–C and C–H stretching modes, and its wide spectral range enable complete vibrational characterization of submonolayer coverages of adsorbed hydrocarbons.[13] The dipole selection rule constraint in IR, IRAS, and HREELS can be broken in HREELS by performing off-specular scans so that all vibrational modes can be observed. This is important in species identification, and critical in obtaining vibrational frequencies required to generate a molecular force field and in determining adsorption sites.

Conclusions

HREELS is one of the most important techniques for probing physical and chemical properties of surfaces. The future is bright, with new opportunities arising from continued fundamental advances in understanding electron scattering mechanisms and from improved instrumentation, particularly in the more quantitative aspects of the technique.[14] A better understanding of the scattering of electrons from surfaces means better structure determination and better probe of electronic properties. Improvements are coming in calculating HREELS cross sections and surface phonon properties and this means a better understanding of lattice dynamics. Extensions of dielectric theory of HREELS could lead to new applications concerning interface optical phonons and other properties of superlattice interfaces.

Novel applications of the HREELS technique include the use of spin-polarization of the incident or analyzed electrons and time-resolved studies on the ms and sub-ms time scale (sometimes coupled with pulsed molecular beams) of dynamical aspects of chemisorption and reaction. Studies of nontraditional surfaces, such as insulators, alloys, glasses, superconductors, model supported metal catalysts, and "technical" surfaces (samples of actual working devices) are currently being expanded. Many of these new studies are made possible through improved instrumentation. While the resolution seems to be limited practically at 10 cm^{-1}, higher intensity seems achievable. Advances have been made recently in the monochromator, analyzer, lenses, and signal detection (by using multichannel detection). New configurations, such as that utilized in the dispersion compensation approach, have improved signal levels by factors of 10^2–10^3.

Related Articles in the Encyclopedia

EELS, IR, FTIR, and Raman Spectroscopy

References

1 H. Ibach and D. L. Mills. *Electron Energy Loss Spectroscopy and Surface Vibrations*. Academic, New York, 1982. An excellent book covering all aspects of the theory and experiment in HREELS.

2 W. H. Weinberg. In: *Methods of Experimental Physics.* **22,** 23, 1985. Fundamentals of HREELS and comparisons to other vibrational spectroscopies.

3 *Vibrational Spectroscopy of Molecules on Surfaces.* (J. T. Yates, Jr. and T. E. Madey, eds.) Plenum, New York, 1987. Basic concepts and experimental methods used to measure vibrational spectra of surface species. Of particular interest is Chapter 6 by N. Avery on HREELS.

4 *Vibrations at Surfaces.* (R. Caudano, J. M. Gilles, and A. A. Lucas, eds.) Plenum, New York, 1982; *Vibrations at Surfaces.* (C. R. Brundle and H. Morawitz, eds.) Elsevier, Amsterdam, 1983; *Vibrations at Surfaces 1985.* (D. A. King, N. V. Richardson and S. Holloway, eds.) Elsevier, Amsterdam, 1986; and *Vibrations at Surfaces 1987.* (A. M. Bradshaw and H. Conrad, eds.) Elsevier, Amsterdam, 1988. Proceedings of the International Conferences on Vibrations at Surfaces.

5 B. E. Koel, B. E. Bent, and G. A. Somorjai. *Surface Sci.* **146,** 211, 1984. Hydrogenation and H, D exchange studies of $CCH_{3(a)}$ on Rh (111) at 1-atm pressure using HREELS in a high-pressure/low pressure system.

6 P. Skinner, M. W. Howard, I. A. Oxton, S. F. A. Kettle, D. B. Powell, and N. Sheppard. *J. Chem. Soc., Faraday Trans.* **2,** 1203, 1981. Vibrational spectroscopy (infrared) studies of an organometallic compound containing the ethylidyne ligand.

7 M. E. Bartram and B. E. Koel. *J. Vac. Sci. Technol.* **A 6,** 782, 1988. HREELS studies of nitrogen dioxide adsorbed on metal surfaces.

8 M. T. Paffett, S. C. Gebhard, R. G. Windham, and B. E. Koel. *J. Phys. Chem.* **94,** 6831, 1990. Chemisorption studies on well-characterized SnPt alloys.

9 J. A. Gardella, Jr, and J. J. Pireaux. *Anal. Chem.* **62,** 645, 1990. Analysis of polymer surfaces using HREELS.

10 J. J. Pireaux, C. Grégoire, M. Vermeersch, P. A. Thiry, and R. Caudano. *Surface Sci.* **189/190,** 903, 1987. Surface vibrational and structural properties of polymers by HREELS.

11 J. J. Pireaux, M. Vermeersch, N. Degosserie, C. Grégoire, Y. Novis, M. Chtaïb, and R. Caudano. In: *Adhesion and Friction.* (M. Grunze and H. J. Kreuzer, eds.) Springer-Verlag, Berlin, 1989, p. 53. Metallization of polymers as probed by HREELS.

12 P. A. Thiry, M. Liehr, J. J. Pireaux, and R. Caudano. *J. Electron Spectrosc. Relat. Phenom.* **39,** 69, 1986. HREELS of insulators.

13 B. E. Koel. *Scanning Electron Microscopy* **1985/IV**, 1421, 1985. The use of HREELS to determine molecular structure in adsorbed hydrocarbon monolayers.

14 J. L. Erskine. *CRC Crit. Rev. Solid State Mater. Sci.* **13**, 311, 1987. Recent review of scattering mechanisms, surface phonon properties, and improved instrumentation.

8.4 NMR

Solid State Nuclear Magnetic Resonance

HELLMUT ECKERT

Contents

Introduction

Solid state NMR is a relatively recent spectroscopic technique that can be used to uniquely identify and quantitate crystalline phases in bulk materials and at surfaces and interfaces. While NMR resembles X-ray diffraction in this capacity, it has the additional advantage of being element-selective and inherently quantitative. Since the signal observed is a direct reflection of the local environment of the element under study, NMR can also provide structural insights on a *molecular* level. Thus, information about coordination numbers, local symmetry, and internuclear bond distances is readily available. This feature is particularly useful in the structural analysis of highly disordered, amorphous, and compositionally complex systems, where diffraction techniques and other spectroscopies (IR, Raman, EXAFS) often fail.

Due to these virtues, solid state NMR is finding increasing use in the structural analysis of polymers, ceramics and glasses, composites, catalysts, and surfaces.

Examples of the unique insights obtained by solid state NMR applications to materials science include: the Si/Al distribution in zeolites,[1] the hydrogen microstructure in amorphous films of hydrogenated silicon,[2] and the mechanism for the zeolite-catalyzed oligomerization of olefins.[3]

Basic Principles

Nuclear Magnetism and Magnetic Resonance

NMR spectroscopy exploits the magnetism of certain nuclear isotopes.[4–6] Nuclei with odd mass, odd atomic number, or both possess a permanent magnetic moment, which can be detected by applying an external magnetic field (typical strength in NMR applications: 1–14 Tesla). Quantum mechanics states that the magnetic moments adopt only certain discrete orientations relative to the field's direction. The number of such discrete orientations is $2I+1$, where I, the nuclear spin quantum number, is a half-integral or integral constant. For the common case $I = ½$, two distinct orientations (states) result, with quantized components of the nuclear spin parallel and antiparallel to the field direction. Since the parallel orientations are energetically more favorable than the antiparallel ones, the populations of both states are unequal. As a consequence, a sample placed in a magnetic field develops a macroscopic magnetization M_0. This magnetization forms the source of the spectroscopic signal measured.

In NMR spectroscopy the precise energy differences between such nuclear magnetic states are of interest. To measure these differences, electromagnetic waves in the radiofrequency region (1–600 MHz) are applied, and the frequency at which transitions occur between the states, is measured. At resonance the condition

$$\omega = \gamma B_{loc} = \gamma(B_0 + B_{int}) \tag{1}$$

holds, where ω is the frequency of the electromagnetic radiation at which absorption occurs. The strength of the magnetic field present at the nuclei B_{loc} is generally very close to the strength of the externally applied magnetic field B_0 but differs slightly from it due to internal fields B_{int} arising from surrounding nuclear magnetic moments and electronic environments. The factor γ, the gyromagnetic ratio, is a characteristic constant for the nuclear isotope studied and ranges from 10^6 to 10^8 rad/Tesla-s. Thus, NMR experiments are always element-selective, since at a given field strength each nuclear isotope possesses a unique range of resonance frequencies.

Measurement and Observables

Figure 1 shows the detailed steps of the measurement, from the perspective of a coordinate system rotating with the applied radiofrequency $\omega_0 = \gamma B_0$. The sample is in the magnetic field, and is placed inside an inductor of a radiofrequency circuit

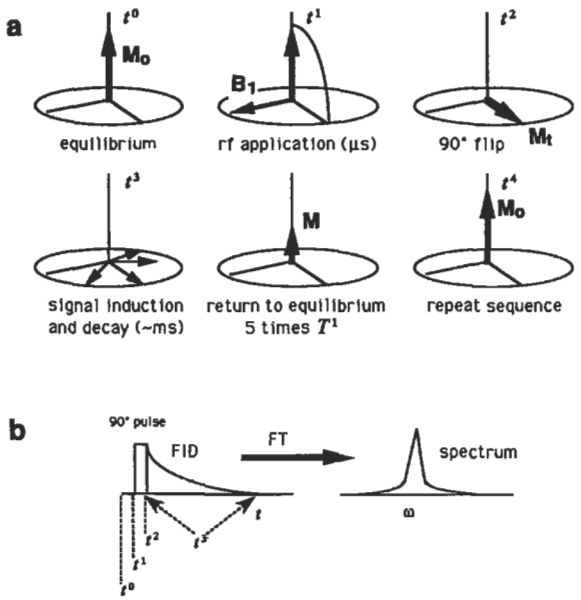

Figure 1 **Detection of NMR signals (a), shown in the rotating coordinate system associated with the oscillating magnetic field component B_1 at the applied radiofrequency ω_0 at various stages (t_0–t_4) of the experiment: t_0, spin system with magnetization (fat arrow) at equilibrium; t_1, irradiation of the B_1 field orthogonal to the magnetization direction tips the magnetization; t_2, the system after a 90° pulse resulting in transverse magnetization M_t; t_3, off-resonance precession and free induction decay in the signal acquisition period following the pulse; and t_4, return to spin equilibrium after spin–lattice relaxation; timing diagram of the experiment (b), followed by Fourier transformation.**

tuned to the resonance frequency of the nucleus under observation. The magnetization present at time t_0 is then detected by applying a short, intense (100–1000 W) radiofrequency pulse (typically 1–10 μs) in a direction perpendicular to B_0 (t_1). The oscillating magnetic component of the radiofrequency pulse stimulates transitions between the magnetic states and tips M_0 into the plane perpendicular to the direction of the magnetic field (90° pulse, t_2). Following this pulse, the magnetization oscillates in this plane at the transition frequency ω and also decays in time due to the various internal interactions present (t_3). It thereby induces an ac voltage signal in a coil, which is amplified, digitized, and acquired over a typical period of several ms (t_3). Fourier transformation of this free induction decay (FID) signal then results in the *NMR spectrum*, a plot of absorption intensity versus frequency. The position, width, and shape of the spectral peaks reflect the local fields present at the nuclei due to internal interactions and allow various chemical conclusions. The area under a spectral peak is directly proportional to the number of nuclei contributing to the resonance, and can be used for quantification purposes.

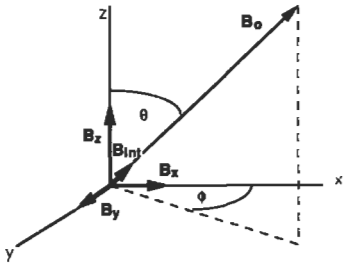

Figure 2 **Schematic illustration of the influence of chemical shift upon NMR spectra. See text for further explanation.**

Since typical NMR signals are quite weak, extensive signal averaging by repetitive scanning is generally necessary. The pulsing rate at which this can occur depends on the time it takes for the spin system to return into its initial state after the 90° pulse, with M_0 along the magnetic field direction (t_4). This process can generally be described by first-order kinetics. The associated time constant T_1, the spin-lattice relaxation time, can vary from a few ms to several hours in solids.

Structural and Chemical Information from Solid State NMR Line shapes

Internal Interactions

What makes NMR so useful for addressing structural questions in solids is the fact that B_{loc}, and hence the resonance frequency ω, are influenced by various types of internal interactions. These are a direct reflection of the local structural and chemical bonding environments of the nuclei studied, and hence are of central chemical interest. Generally, the observed nuclei experience three types of interactions:[6] *magnetic dipole–dipole interactions* with the magnetic moments from other, nearby nuclei; *chemical shift interactions* with the magnetic fields from the electron clouds that surround the nuclei; and (for nuclei with spin > ½) *electric quadrupole interactions* with electrostatic field gradients generated by the chemical bonding environment. Each of these interactions is characterized by a few spectroscopic parameters, which are listed in Table 1. Typically, these parameters are extracted from experimental spectra by computer-fitting methods or are measured by *selective averaging* techniques.

Due to the simultaneous presence of all three interactions, the resulting solid state NMR spectra can be quite complex. Fortunately, however, in many cases one interaction mechanism is dominant, resulting in spectra that yield highly specific information about local symmetry and bonding. In the following, we will discuss an application of the chemical shift anisotropy. Figure 2 illustrates that the anisotropic interaction between the molecule and the externally applied magnetic field

Interaction	Parameters	NMR measurement	Structural significance
Chemical shift (isotropic component)	δ_{iso}	Magic-angle spinning	Chemical bonding coordination number
Chemical shift anisotropy	δ_{xx}, δ_{yy}, δ_{zz}	Line-shape analysis MAS-sidebands	Coordination symmetry
Dipole–dipole (homonuclear)	M_2(homo) (mean-squared local field)	Spin-echo NMR	Internuclear distances, number of surrounding nuclei
Dipole–dipole (heteronuclear)	M_2(hetero)	Spin-echo double resonance (SEDOR)	
Nuclear electric quadrupole	*QCC* (quadrupole coupling constant), (asymmetry parameter)	Line-shape analysis, nutation NMR	Coordination symmetry

Table 1 **Interactions in solid state NMR, parameters, their selective measurement, and their structural significance.**

induces local magnetic field components B_x, B_y, and B_z along the *x*-, *y*-, and *z*-directions of a molecular axis system. Quite generally, $B_x \neq B_y \neq B_z$. The vector sum of these components produces a resultant B_{int} along the direction of B_0, the axis of quantization, and hence affects the resonance condition. As seen in Figure 2, the magnitude of B_{int} (and hence the resonance frequency) will depend crucially on the orientation (θ, ϕ) of this molecular axis system relative to the magnetic field direction.

In a polycrystalline or amorphous material, the orientational statistics lead to a distribution of resonance conditions. Generally, we can distinguish three situations, illustrated in Figure 3a–c: The spectrum in Figure 3c is observed for compounds with asymmetric chemical environments. It shows three distinct features, which can be identified with the different Cartesian chemical shift components δ_{xx}, δ_{yy}, and δ_{zz} in the molecular axis system. Figure 3b corresponds to the case of cylindrical symmetry, where $\delta_{xx} = \delta_{yy} \neq \delta_{zz}$, and hence only two distinct line shape components appear. Finally, for chemical environments with spherical symmetry the chemical shift is the same in all three directions. Accordingly, the solid state NMR spectrum consists of only a single peak (see Figure 3a). The values of δ_{ii} extracted

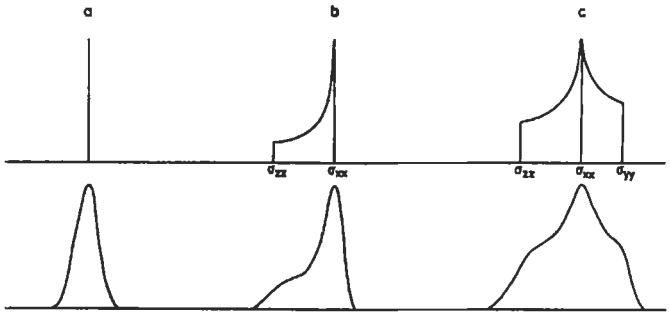

Figure 3 **Characteristic solid state NMR line shapes, dominated by the chemical shift anisotropy. The spatial distribution of the chemical shift is assumed to be spherically symmetric (a), axially symmetric (b), and completely asymmetric (c). The top trace shows theoretical line shapes, while the bottom trace shows "real" spectra influenced by broadening effects due to dipole–dipole couplings.**

from the spectra usually are reported in ppm relative to a standard reference compound. By definition,

$$\delta_{ii}[\text{ppm}] = 10^6 \cdot \frac{\omega_{ii} - \omega_{ref}}{\omega_0} \tag{2}$$

An Example: Chemical Shift Anisotropy in Solid Vanadium Compounds

Figure 4 shows representative solid state ^{51}V NMR spectra of crystalline vanadates. Each model compound typifies a certain local vanadium environment with well-defined symmetry as shown. One can see from these representative data that the solid state ^{51}V chemical shift anisotropies are uniquely well suited for differentiating between the various site symmetries. VO_4^{-3} groups with approximate spherical symmetry yield single-peak spectra, dimeric $V_2O_7^{-4}$ groups (which possess a three-fold axis and hence cylindrical symmetry) yield spectra resembling Figure 3b, while the spectra of the completely asymmetric $VO_{2/2}O_2^-$ groups are of the kind shown in Figure 3c. Highly diagnostic line shapes are also observed for vanadium in distorted octahedral environments (ZnV_2O_6) and in square-pyramidal environments (V_2O_5).

An Application: ^{51}V NMR of V oxide films on metal oxide supports

Investigations carried out within the past few years have revealed that multicomponent metal oxide systems may interact at interfaces by having one component form a two-dimensional metal oxide overlayer on the second metal oxide component. For example, vanadium oxide can be dispersed on TiO_2, ZrO_2, SiO_2, Al_2O_3, and

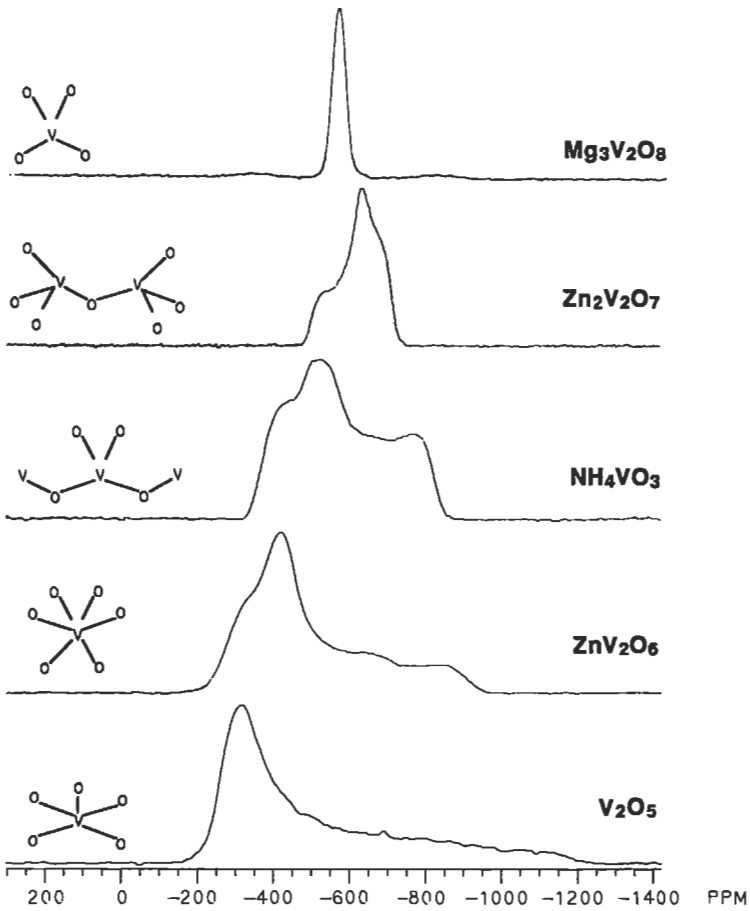

Figure 4 **Local microstructures and experimental solid state ^{51}V NMR spectra in crystalline vanadium oxide compounds.**

other oxide supports by impregnating the latter with a liquid molecular precursor and following with calcination. Many of these systems are potent oxidation catalysts, with significant inherent advantages to bulk V_2O_5. To explore a relationship between the catalytic activity and structural properties, extensive solid state ^{51}V NMR studies have been carried out on these phases.[8] These studies have benefited greatly from the chemical shift systematics discussed above. Figure 5 shows experimental spectra of V surface oxide on γ-Al_2O_3 support. In conjunction with the model compound work one can conclude that two distinctly different vanadia species are present at the surface: At low vanadia contents, a four-coordinated chain-type species dominates, whereas with increasing surface coverage a new site emerges whose spectroscopic parameters reveal the presence of a distorted octahedral vanadium environment. Similar trends have been seen with other metal oxide supports,

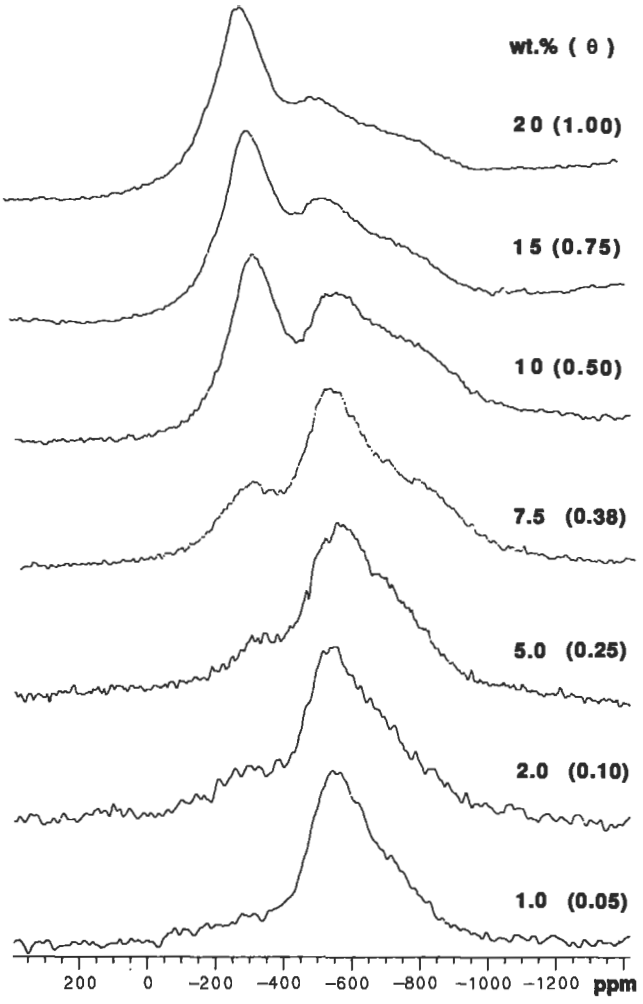

Figure 5 **Solid state ^{51}V NMR spectra of Vanadium oxide on γ-alumina as a function of vanadium loading (wt.%) and surface coverage θ. Note the gradual emergence of the six-coordinated vanadium site with increased loading.**

although the type of vanadium environment in the overlayer also depends strongly on the acidity of the surface.

Selective Averaging Techniques

In general, the specific information that can be obtained from a simple solid state NMR experiment depends on the "personality" of the nuclear isotope under study. In many cases, solid state NMR spectra are not as straightforwardly interpretable as in the preceding example. Furthermore, disordered materials, such as thin films,

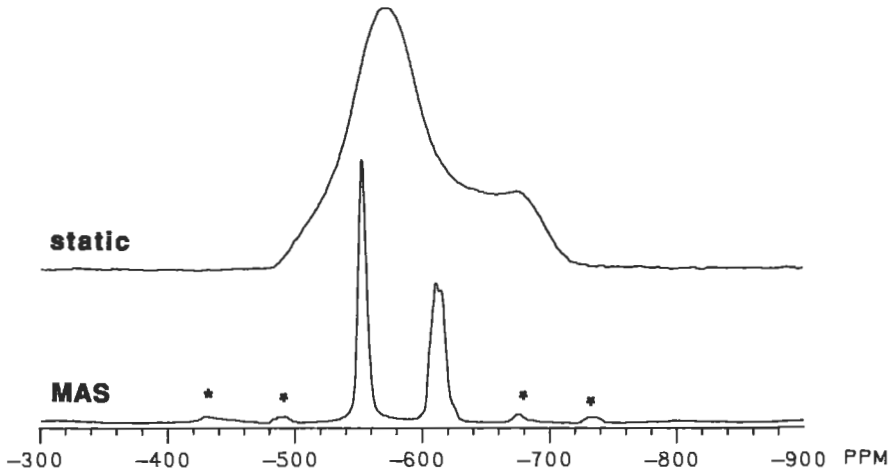

Figure 6 **Solid state ^{51}V static and magic-angle spinning NMR spectra of α-$Mg_2V_2O_7$. This compound has two crystallographically distinct vanadium sites. While the static spectrum is a superposition of two powder patterns of the kind shown in Figure 3, MAS leads to well-resolved sharp resonances. Weak peaks denoted by asterisks are spinning sidebands due to the quadrupolar interaction.**

glasses, and composites, often show only broad and unresolved spectra, because in such samples the spectroscopic parameters are subject to distribution effects. Here, the diagnostic character of solid state NMR can be enhanced dramatically by selective averaging techniques. The idea is to simplify the spectra by suppressing certain interactions while preserving others for analysis. The most popular and most widely applied experiment is to acquire the NMR spectrum while rotating the sample rapidly about an axis inclined by 54.7° (the "magic" angle) relative to the magnetic field direction. This technique, called Magic-Angle Spinning (MAS), results in an average molecular orientation of $\theta = 54.7°$ relative to the magnetic field over the rotation period, regardless of the initial molecular orientation. Theory predicts that at this specific angle the anisotropy of all internal interactions (which scale with the factor $3\cos^2\theta-1$) vanishes. Consequently, MAS converts broad powder patterns of the kind shown in Figure 3a–c into highly resolved sharp resonances that can be straightforwardly assigned to individual sites. For example, Figure 6 illustrates the superior ability of MAS to resolve the crystallographically distinct vanadium sites in the model compound α-$Mg_2V_2O_7$. The high resolution obtained by MAS and the simplicity of the spectra make solid state NMR a particularly useful technique for identifying crystalline phases in the bulk or at surfaces and interfaces.

A number of other, more sophisticated, selective averaging tools (including spin echo, double resonance and two-dimensional techniques) are available, both for spectral editing purposes and for obtaining quantitative information about inter-

atomic distances.[7] However, among all these techniques, the conceptually simple MAS-NMR experiment has had by far the biggest impact in materials science applications.

Instrumentation

NMR instrumentation consists of three chief components: a magnet, a spectrometer console, and a probe. While in the past much solid state NMR research was conducted on home-built equipment, the current trend is toward the acquisition of commercial systems. The magnets used for solid state NMR applications generally are superconducting solenoids with a cylindrical bore of 89-mm diameter. The most common field strengths available, 4.7, 7.0, 9.4, and 11.7 Tesla, correspond to proton resonance frequencies near 200, 300, 400, and 500 MHz, respectively.

The spectrometer console comprises a radiofrequency part for the generation, amplification, mixing, and detection of radiofrequency and NMR signals, and a digital electronics part, consisting of a pulse programmer, a digitizer, and an on-line computer. Equipment normally used for pulsed liquid state NMR applications often can be modified for solid state experiments by adding high-power amplifiers (up to 1-kW output power) and fast digitizers (2 MHz or faster).

NMR probes are used to transfer the radiofrequency pulse to the sample and to detect the nuclear induction signal after the pulse. They contain radiofrequency circuitry, which is tunable to the nuclear resonance frequency via variable capacitors and which is based usually on a single solenoidal coil (diameter 4–25 mm). MAS-NMR experiments require special probes, enabling fast sample rotation within the magnet. Currently, MAS is done mostly on powdered samples packed within cylindrical containers (rotors) that are machined from single-crystal alumina, zirconia, or silicon nitride to precise dimensions. High-pressured gases (air, N_2, or Ar, at 40–60 lb/in^2) thrusting on turbine-shaped caps are used to accomplish fast rotation. For routine experiments, typical spinning speeds are 5–10 kHz; with suitable equipment up to 20 kHz can be reached.

Practical Aspects and Limitations

Sample preparation requirements in solid state NMR are strikingly simple because the measurement is carried out at ambient temperature and pressure. Wide-line NMR experiments can be carried out on solid samples in any form, as far as the sample dimensions fit those of the coil in the NMR probe. MAS experiments require the material to be uniformly distributed within the rotor.

Compared to other spectroscopic methods, NMR spectroscopy is a very insensitive technique. As a general rule of thumb, the sample studied must contain at least 10^{-5} moles of target nuclei. The required sample size thus depends on the percentage of the element present in the sample, as well as on the natural abundance of the

NMR isotope measured. For example, for the detection of phosphorus by ^{31}P NMR in a sample containing 3 wt.% phosphorus, approximately 10 mg of sample are required. By contrast, the corresponding detection limit for ^{29}Si in a similar situation is 22 times higher, due to the much lower natural abundance (4.7%) of the ^{29}Si isotope.

Naturally, the low sensitivity poses a particular obstacle to NMR studies of thin films and surfaces. Large surface areas are obviously favorable (the samples in Figure 5 have surface areas around 150 m^2/g), but good results can often be obtained on samples with surface areas as small as 10 m^2/g. Experimentally, the detection sensitivity can be increased by increasing the applied field strength; by increasing the sample size (although practical considerations often impose a maximum sample volume of several cm^3); and by using special NMR techniques (cross-polarization[4–6]) for sensitivity enhancement.

Additional limitations arise from the nuclear electric quadrupole interaction for nuclei with $I > ½$ and from the dipolar interaction of nuclei with localized electron spins in paramagnetic samples. Both interactions tend to interfere with the alignment of the nuclear spins in the external magnetic field, and to make the observation of NMR signals difficult. Due to these factors, less than half the elements in the periodic table are conducive to solid state NMR experiments. The following ranking holds with regard to detection sensitivity and general suitability in the solid state—highly favorable elements: H, Li, Be, B, F, Na, Al, P, V, Sn, Xe, Cs, Pt, and Tl; less well-suited elements, where NMR often suffers from sensitivity restrictions: C, N, Si, Se, Y, Rh, Ag, Cd, Te, W, Hg, and Pb; and elements whose suitability is often limited by quadrupolar interactions: N, O, Cl, Mn, Co, Cu, Ga, K, Rb, Nb, Mo, In, and Re. Elements not listed here can be considered generally unsuitable for solid state NMR.

Quantitative Analysis

In contrast to other spectroscopies, such as IR/Raman or VIS/UV, NMR spectroscopy is inherently quantitative. This means that for a given nucleus the proportionality factor relating the area of a signal to the number of nuclei giving rise to the signal is not at all sample-dependent. For this reason, NMR spectroscopy has been used extensively for absolute and relative quantitation experiments, using chemically well-defined model compounds as standards.

It is essential, however, to follow a rigorous experimental protocol for such applications. To maintain the quantitative character of NMR spectroscopy, the repetition rate of signal averaging experiments has to be at least five times the longest spin-lattice relaxation time present in the sample. This waiting period is necessary to ensure that the magnetization is probed in a reproducible state, corresponding to thermodynamic equilibrium.

Conclusions

To date, the simple one-pulse acquisition experiments (with or without MAS) reviewed here have been the mainstay for the majority of NMR applications in materials science. A current trend is the increasing use of NMR for *in situ* studies, using more sophisticated hardware arrangements.[3, 9] For the near future, a rapid diffusion of NMR know-how and methodology into many areas of solid state science can be foreseen, leading to the application of more complicated techniques that possess inherently greater informational content than MAS-NMR. Examples of this kind include multiple pulse techniques, such as one- and two-dimensional versions of spin-echo and double resonance methods, and experiments involving variable rotation angles.[7]

Also, new areas for applications are opening up. A most recent development has been the successful demonstration of three-dimensional imaging of ceramic and polymeric materials by solid state NMR techniques. This area is most likely to expand considerably.

Related Articles in the Encyclopedia

EXAFS, FTIR, XRD

References

1 J. Klinowski. *Prog. NMR Spectrosc.* **16,** 237, 1984. A summary of ^{29}Si MAS-NMR applications to zeolites.

2 J. Baum, K. K. Gleason, A. Pines, A. N. Garroway, and J. A. Reimer. *Phys. Rev. Lett.* **56,** 1377, 1986. Detection of hydrogen clustering in amorphous hydrogenated silicon by a special technique of dipolar spectroscopy, multiple-quantum NMR.

3 J. F. Haw, B. R. Richardson, I.S. Oshiro, N.D. Lazo, and J. A. Speed. *J. Am. Chem. Soc.* **111,** 2052, 1989. *In situ* NMR studies of catalytic properties.

4 T. M. Duncan and C. R. Dybowski. *Surf. Sci. Rep.* **1,** 157, 1981. An excellent review of relevant NMR theory, modern techniques, and applications to surfaces.

5 B. C. Gerstein and C. R. Dybowski. *Transient Techniques in NMR of Solids.* Academic Press, 1985. An in-depth treatment of the theoretical foundations of solid state NMR.

6 M. Mehring. *Principles of High Resolution NMR in Solids.* Springer Verlag, New York, 1983. An in-depth treatment of the theoretical foundations of solid state NMR.

7 H. Eckert. *Ber. Bunsenges. Phys. Chem.* **94,** 1062, 1990. A recent review of modern NMR techniques as applied to various Materials Science problems.

8 H. Eckert and I. E. Wachs. *J. Phys. Chem.* **93,** 6796, 1989. ^{51}V NMR studies of vanadia-based catalysts and model compounds.

9 J. F. Stebbins and I. Farnan. *Science.* **245,** 257, 1989. Highlights *in situ* NMR applications at ultrahigh temperatures.